FINAL REPORT

for

Period Ending March 31, 1965

Contract No. NASr-73

"Investigation of Unique Gas Permeability Cell System to Remove CO_2 and Other Noxious Gases from Spacecraft Cabins"

To

National Aeronautics and Space Administration

By

Coleman J. Major
Department of Chemical Engineering
University of Iowa
Iowa City, Iowa

ABSTRACT

Several prototypes of a gas permeability cell were constructed using Dow Corning Silastic RTV-501 silicone rubber as the semipermeable membrane. This polymer has a carbon dioxide to oxygen separation factor of approximately 5 at room temperature. This is based on a pure gas permeability rate of 3000 barrer for CO_2 and 600 barrer for O_2. Pure gas permeability measurements also revealed that the carbon dioxide permeability rate is constant over the temperature range 0°-50°C while the oxygen rate is directly proportional to temperature. This indicates that better separation factors are possible at the lower temperatures.

The cell prototypes which were constructed were tested on their ability to separate dilute mixtures of carbon dioxide in oxygen. Constant temperature runs of 40°, 25°, and 0°C were made using feed compositions ranging from 1% - 10% CO_2. A vacuum driving force of approximately 750 mm Hg was used to initiate and maintain the separation process. The cells were found to be somewhat pressure sensitive and ruptured under pressures greater than 5 psia on the high pressure side of the membrane. Only single pass measurements were made. It was observed that a cascade system is required for permeability

separations wherein a nearly complete separation is required. This was attributed to the small magnetude of the separation ratio.

The Weller Steiner Case I model for perfect mixing was used to correlate the experimental results with those obtained using theoretical considerations. Fairly good correlation was found between theoretical and actual data.

CONTENTS

Subject	Page
Summary	1
Introduction	4
Theory	9
Cell Construction	12
Cell Operation	22
Description of Apparatus	26
Film Preparation and Testing	26
Substrate Testing	30
Cell Testing	32
Experimental Procedure	36
Permeabilities of Silicone Rubber Films	36
Substrate Porosities	37
Laminating	37
Cell Construction	38
Testing the Cell	41
Discussion of Results	45
Cell Membranes	45
Substrates and Porosity	50
Cell Assemblies	53
Conclusions	59
Appendix	62
Tables	63
Figures	75
Calculations	89
Nomenclature	93
Bibliography	101

FIGURES

Figure Number	Title	Page
1	Schematic Separation by Selective Permeation	10
2	Graphic Representation of Cell Assembly	17
3	Sectional View of Potted Cell	18
4	Structure of Cell Member and Cell Assembly	20
5	Compact Gas-Permeability Apparatus	27
6	Schematic Substrate Porosity Apparatus	29
7	Substrate Sample Holder	31
8	Schematic Cell Testing Apparatus	33
9	Permeability of RTV-501 Silicone Rubber	48
10	Permeability of RTV-502 Silicone Rubber	49
11	Separation Curves (40°C) (O_2-CO_2) (Cell 3A)	75
12	Separation Curves (25°C) (O_2-CO_2) (Cell 3A)	76
13	Separation Curves (0°C) (O_2-CO_2) (Cell 3A)	77
14	Actual and Theoretical Separation Curves (25°C)	78
15	Apparatus for Measuring Substrate Capacity	80
16	Substrate Capacity for Test Assemblies	81
17	Flow Capacity for Unlaminated Substrates	81
18	Barometric Permeability Apparatus	82
19	Volumetric Compact Permeability Apparatus	83
20	Early Permeation Assemblies	84
21	Permeability Cells	85
22	Permeability Cell in Water Bath	86
23	Cell Testing Apparatus	87
24	Cell Testing Apparatus	87
25	Separation Cell	95
26	View of Layered Assembly	96

TABLES

Table		Page
1	Permeability of Silicone Films	46
2	Substrate Porosity	51
3	Laminated Substrate Porosity	51
4	Typical Data from Permeability Measurement	63
5	Typical Data from Substrate Porosity Measurement	64
6	Cell Separation Test (40°C)(9.8% CO_2 in Feed)	65
7	Cell Separation Test (40°C)(7% CO_2 in Feed)	66
8	Cell Separation Test (40°C)(1% CO_2 in Feed)	67
9	Cell Separation Test (25°C)(8% CO_2 in Feed)	68
10	Cell Separation Test (25°C)(6% CO_2 in Feed)	69
11	Cell Separation Test (25°C)(2% CO_2 in Feed)	70
12	Cell Separation Test (25°C)(9% CO_2 in Feed)	71
13	Cell Separation Test (0°C)(4.5% CO_2 in Feed)	72
14	Cell Separation Test (0°C)(2% CO_2 in Feed)	73
15	Typical Data for Permeability Cell Separation	74
16	Capacity of Permeability Cell Substrate	79
17	Computer Program Weller-Steiner Case I	99

SUMMARY

An investigation into a proposed new design for a gas permeability cell was conducted. This cell was specifically designed to remove and concentrate the carbon dioxide produce in the environments of manned space craft. The investigation included experimental studies of the materials and techniques required for the construction of the cell, fabrication of a prototype of the cell, and experimental tests on the prototype to determine its operating characteristics.

The basic shape of the new cell is that of a multilayer Greek cross. Each layer of the assembly is an individual separation unit. The cross shape permits these individual units to be connected in parallel with the interconnections being made internally. This arrangement greatly facilitates the admittance and withdrawal of the various gas streams while exposing relatively large surface areas to the permeating gases in a comparatively small volume.

Dow Corning Silastic RTV-501 silicone rubber was used for the permeable membrane of the cell. Its permeability to carbon dioxide at 23°C was measured at approximately:

$$3000 \times 10^{-10} \left(\frac{\text{Std cc}}{\text{sec}}\right) \left(\frac{\text{cm}}{\text{cm}^2 \text{cm Hg}}\right)$$

This rate is approximately 5.0 times that of oxygen for the same conditions. Films with a thickness of 0.0058 cm were prepared for this polymer, but films 0.0206 cm thick were used in the actual cell construction to eliminate any possibility of a discontinuity forming.

Ordinary Nibroc brown paper towel, manufactured by the Brown company was selected for the supporting substrate. It demonstrated good porosity properties which were retained after laminating. In the cell which was tested a flow of (105 $ft.^3/min$ $ft./ft.^2$) of air was obtained using a pressure drop of 100 mm Hg through the unlaminated substrate. For the laminated substrates a flow rate of approximately (15.75 $ft.^3/min$ $ft./ft.^2$) was obtained with the same pressure drop. This indicated that channeling occurs across the surface of the unlaminated substrate.

A new process for laminating the film to the substrate was developed. This process involved a partial polymerization of the film before the application of the substrate.

A number of cells were constructed and tested. A typical cell, 3A, contained 8 layers and 16 film surfaces which had a combined film surface of 640 cm^2. It was tested at 0°, 25°, and 40° centigrade

isotherms with various binary mixtures of carbon dioxide in oxygen ranging from 1 to 10 per cent CO_2. A vacuum was used to create the partial pressure driving force across the membranes. The data were plotted as the ratio of (product/feet) vs. concentration of CO_2 in the product stream. Smooth curves resulted which seemed to be representative of those predicted by the Weller Steiner equations. It was concluded that the proposed new permeability cell design is definitely feasible.

INTRODUCTION

The Problem

The removal of carbon dioxide and other noxious vapors from the oxygen support system of a space craft is a formidable problem in manned space exploration. This is particularly so for flights of long duration, and in those instances when a significant number of astronauts are involved in the flight. However, since manned space flights are desirable, several different air purification systems have been proposed.

Of the systems proposed, the gaseous diffusion system incorporates several attractive features.

1. The gaseous diffusion system utilizes a barrier having a selective permeability with respect to carbon dioxide. Thus it operates entirely in the gas phase region. Also, since the driving force is a partial pressure gradient, the system is independent of gravity, and therefore unaffected by the conditions of weightlessness.
2. Theoretically the gaseous diffusion system is a continuous operation. As such, the selective barriers do not need to be recharged or regenerated in order to continue producing a separation.
3. The membranes or selective barriers of such systems are chemically inert and stable over a

relatively wide temperature range.

Permeability or gaseous diffusion systems also have several disadvantages.

1. Permeability separations require relatively high pressure drops for most selective barriers. This means that the power requirements for interstage compression could be prohibitive for the power systems of small space craft.

2. Theoretically a diffusion system cannot provide a complete separation in a single pass. This means that a cascade system would be necessary in order to provide sufficient capacity. The volume requirements for a cascade system could become excessive for space craft use.

Having reviewed both the advantages and disadvantages of a system, it becomes necessary to weigh the sum of the one against that of the other. Quite often new techniques are devised to overcome the disadvantages of a system and thereby make it appear more feasible. In this particular instance, considerable attention has been given to the application of selective membranes to remove carbon dioxide in submarines and manned space capsules. The possibility of success for these applications, however, has been seriously hampered by the inability to overcome the previously mentioned

disadvantages of such a system. In most cases the lack of a workable large-area small-volume permeation cell has been especially troublesome. It is believed, however, that the proposed cell design will answer this and many of the other shortcomings associated with the present units. Also, it may possibly demonstrate that the removal of carbon dioxide from respiratory air in small enclosed spaces by selective permeation is in fact, operationally feasible.

The Proposal

One of the classical methods of obtaining a large surface area per unit volume is that exhibited by a tube bundle in a heat exchanger. For the proposed new design, alternating thin layers of a selective plastic membrane and a porous substance will replace the tubes in the heat exchanger model. Figures 2 and 3. The unique feature of this design is the manner in which interconnection between alternate compartments is accomplished. This technique enables hundreds or thousands of individual cell compartments to be connected in parallel without complicated assembly operations. The design also lends itself to construction of rigid hermetically sealed units similar to the potted components used in the electronics industry.

Before a successful cell could be built, however, a

number of variables had to be studied, and several manufacturing techniques had to be developed. To accomplish this a plan of study was proposed and followed. It is briefly summarized in the following paragraphs.

1) Every effort was made to establish which materials were best suited for cell construction. This included permeability tests on a number of selective membranes, and permeability tests on samples of the porous medium which was to be used between the successive layers of the selective membranes. These latter permeability tests were conducted with edge-wise flow instead of the usual right angle flow. This helped to determine whether or not the pressure drop through that particular porous medium would be excessive.

2) Beginning with the best construction materials, techniques were developed for coating the porous medium with a thin film of the plastic membrane. Tests were then devised to determine the minimum practical thickness for the laminated film. Permeability tests of the film laminated to the porous medium were also conducted. The principle point here was to make sure that a continuous film had been formed and that the polymer had not penetrated the porous medium sufficiently to clog its pores.

3) Experiments were conducted to determine the best procedures for assembling a cell unit. This included tests on the drilling operation for cutting the holes to inter-connect the alternate layers, tests on procedures for bonding the individual layers to one another, and experiments with potting materials to be used for potting the cells.

4) When a method for constructing the cell had been perfected, a hand-assembled unit was built and tested.

In the following report each of the steps just described will be discussed in detail. The results obtained from the various tests performed in each step will also be presented, and wherever possible they will be compared with the results obtained from purely theoretical considerations.

THEORY

Introduction

The proposed permeability cell is a process for separating gaseous mixtures by permeation through a semi-permeable membrane. Since it is a separation process, the membrane must demonstrate a different selectivity for each of the gaseous components being separated. Moreover, for a separation by permeation it is essential that every membrane used be completely non-porous. If this is not so, and the membrane contains pin holes or other microscopic defects which destroy the continuity of the film, then the selectivity of the film will also be lost. Consequently, any resulting separation which is obtained will not be by permeation, but rather by diffusion or some other less selective process.

For a single stage unit, a permeability separation requires four basic steps. Figure 1.

1. The gaseous misture must be brought into contact with one side of the semi-permeable membrane. The contact between gases and membrane results in the absorption and dissolution of the gases, thereby causing a partial pressure gradient to develop across the membrane.
2. Under the influence of the partial pressure

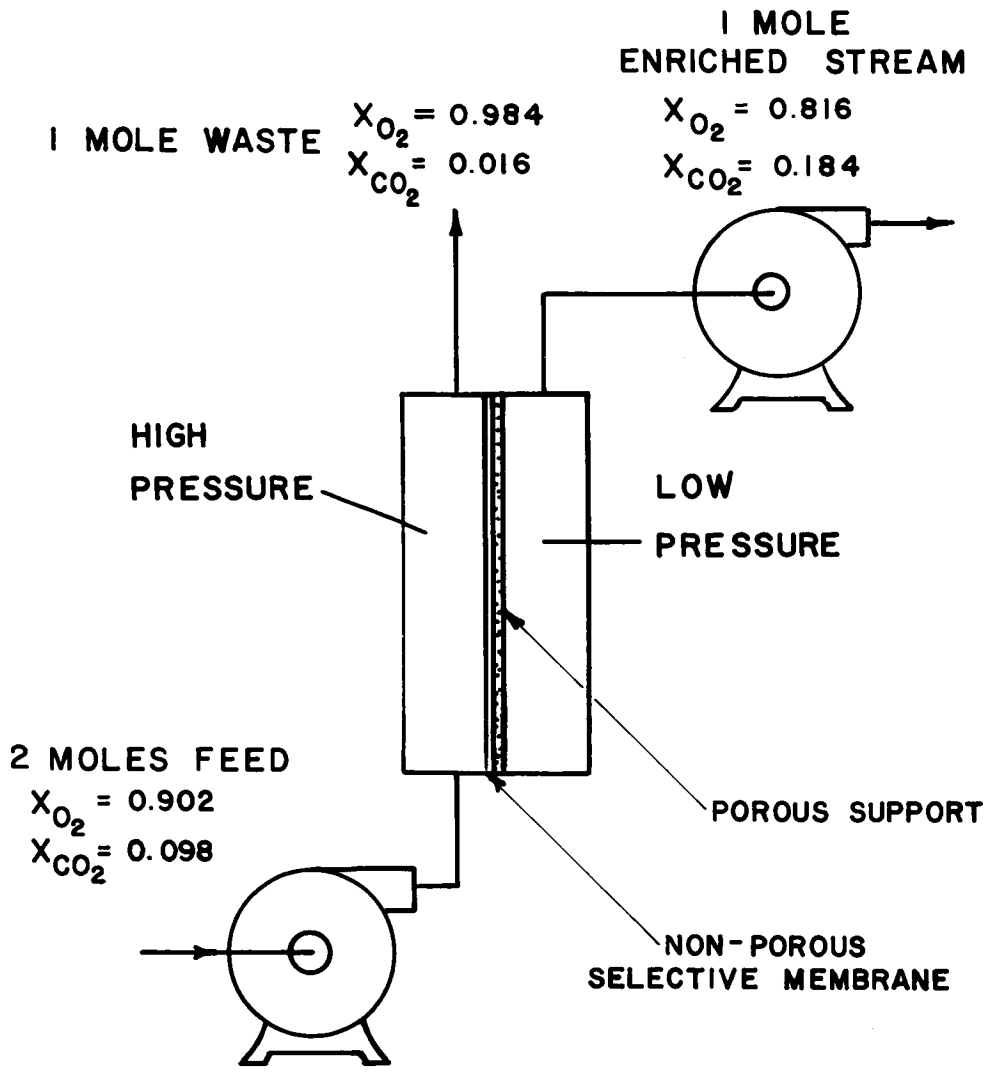

FIGURE I. SCHEMATIC
SEPARATION BY SELECTIVE PERMEATION

gradient, the gases will begin to permeate the membrane. The direction of permeation is through the membrane from the high pressure side to the low pressure side. The rate of permeation for each component of the mixture will be governed by the selective properties of the film and by the magnetude of the partial pressure gradient.

3. The permeated gas, now enriched in at least one of the components, is evaporated from the low pressure side of the membrane and removed as product from the system. The removal of the product stream is necessary to sustain the partial pressure gradient across the membrane.
4. The unpermeated and depleted gas is similarly removed as waste from the high pressure side of the system

Three of these four steps are problems involving the transportation of gases to and from the selective membrane. Consequently all three may be treated in similar manners during the design and construction of a permeability cell. The step involving the actual separation process produces a greater variety of problems, however, and must be treated much more rigorously. All four steps will be examined to some degree in the following theoretical discussion on cell construction.

Cell Construction

From the preceding discussion it is evident that the selective membrane is the most fundamental part of a permeability cell. Therefore it is reasonable to expect that the most selective and permeable membrane available would be an integral part of any proposed cell design. With this purpose in mind, experiments have been divised to test and compare the performances of potential membranes. It has been demonstrated for instance, that the permeability and selectivity of a membrane is proportional to the membrane's permeability coefficient. This coefficient is different for each gas and varies with temperature according to the Arrenhius relationship. (8) (11) Its magnetude determines the ease and the degree to which a gas will permeate through the film; the larger the coefficient the greater will be the rate of permeation through the membrane. Because the permeability coefficient is so descriptive of the membrane's permeability properties, it serves as a criterion for evaluating potential membranes, and its accurate evaluation is very important.

The gas permeability coefficient for a film is defined as the volume of a pure gas flowing normal to two parallel surfaces a unit distance (thickness) apart, under steady conditions, through unit area under unit

pressure differential, at a stated test temperature. As such the coefficient is a basic property of the material and independent of specimen geometry. It is related to the diffusion rate and to the solubility of a gas by the equation; (11)

$$\bar{P} = DS$$

where $\bar{P}$ = gas permeability coefficient

D = diffusion rate

S = solubility

An accepted unit of $\bar{P}$ is 1 cm^3 (at standard conditions) per sec, cm^2, cm of mercury (pressure) per cm. of thickness at the stated temperature of the test. A convenient unit is the barrer:

$$\bar{P}\ (\text{barrer}) = \frac{10^{-10} cm^3\ (STP)\ cm}{sec.\ \ cm^2\ cmHg}$$

In order to determine the relative rate of separation of a binary mixture, one must first find the ratio of the gas permeability coefficients for the temperature at which the separation is to take place. If this ratio is greater or less than unity, a separation of the mixture is possible, and the rate of separation will be proportional to the relative magnetude of the ratio. If the conditions are such that the ratio obtained is equal to unity, then the mixture will not separate, but will behave as an azeotropic mixture.

The magnetude of the permeability coefficient, i. e. 10^{-10}, reveals that the flow rates associated with permeation are quite small. A dimensional analysis of the coefficient suggests, however, three possible methods of designing a cell to compensate for these small rates. Thus (1) if the thickness of the film is decreased, (2) the permeation area increased, (3) or the partial pressure drop increased, then the total amount of permeated gas must increase. In order to produce the most effective separation, the ideal cell design should include a combination of all three of these possibilities for increasing the permeation rate.

Of the three possibilities, the partial pressure gradient is not a function of cell construction. It is rather, a function of the operating conditions of the cell. As such, it is limited to the amount and type of power which is available for operating a cell assembly. Thus the partial pressure gradient could range in magnetude from those produced by vacuum forces to those created with compressive pressures from pumps. For this reason the cell should be designed to operate over as wide a pressure range as possible, thereby achieving a maximum flexibility.

The remaining two possibilities, film thickness and permeation area, are definitely construction features.

As such they may be incorporated into the basic cell design as construction conditions permit.

The dimensional analysis of the permeability coefficient revealed that the permeation rate increased as the thickness of the film decreased. This implies that the thinnest possible film is the most desirable for cell construction. A minimum in the film thickness is reached either through limitations in the method of preparation, or through limitations in the film itself. It will be recalled that a selective film must be everywhere continuous in order to produce a separation. Using this requirement of continuity as a criterion, thinner and thinner films can be prepared until a thickness is reached at which the film begins to show discontinuities. This thickness then becomes the limiting thickness of the film. For some polymers, however, it is possible to produce an even thinner film by a process of lamination. In this operation, extremely thin films are prepared irregardless of the number of small discontinuities which may be formed in the process. Two of these super thin films are then laminated together, producing a composite membrane which is still quite thin. Moreover, the resulting membrane is also continuous, since the probability that discontinuities in the two laminated films will coincide is statistically

very small. Thin films produced by these two methods may, however, rupture and fail when they are subjected to the stresses encountered during cell operation. Thus the thickness of the film may have to be increased to add strength and thereby prevent damage. The optimum, between strength and thinness, is obtained through experimentation. The experimental value then becomes the minimum limiting thickness for the film. However, by proper cell design the operating stresses in the cell can be significantly reduced. This then permits a corresponding reduction in the minimum thickness for the film being used.

It will be recalled that the third possibility for increasing the total flow rate through a semi-permeable membrane involved the enlargement of the area which is available for permeation. It appears that the enlargement of this area would be a simple task. And it is. However, this particular possibility differs from the two just described in that an increase in the membrane area also necessitates an increase in the volume of the cell.

Herein lies the difficulty of designing a cell for application in confined spaces: How can large surface areas be assembled into comparatively small volumes? Until this question is satisfactorily answered, the

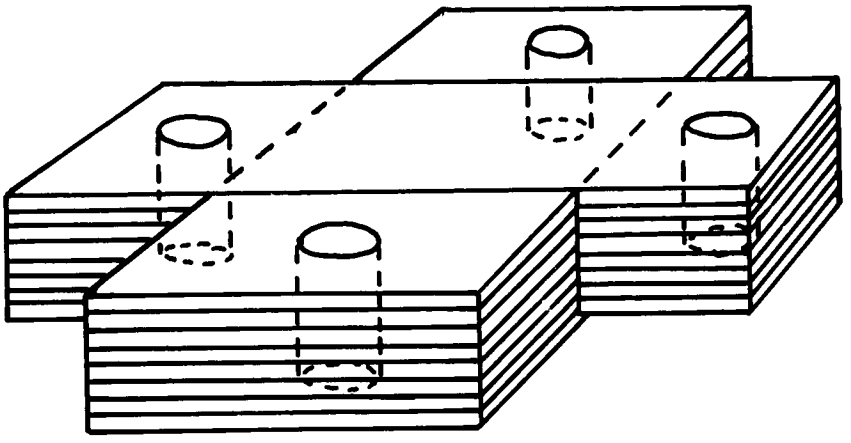

FIGURE 2
GRAPHIC REPRESENTATION OF CELL ASSEMBLY
C.J.M.

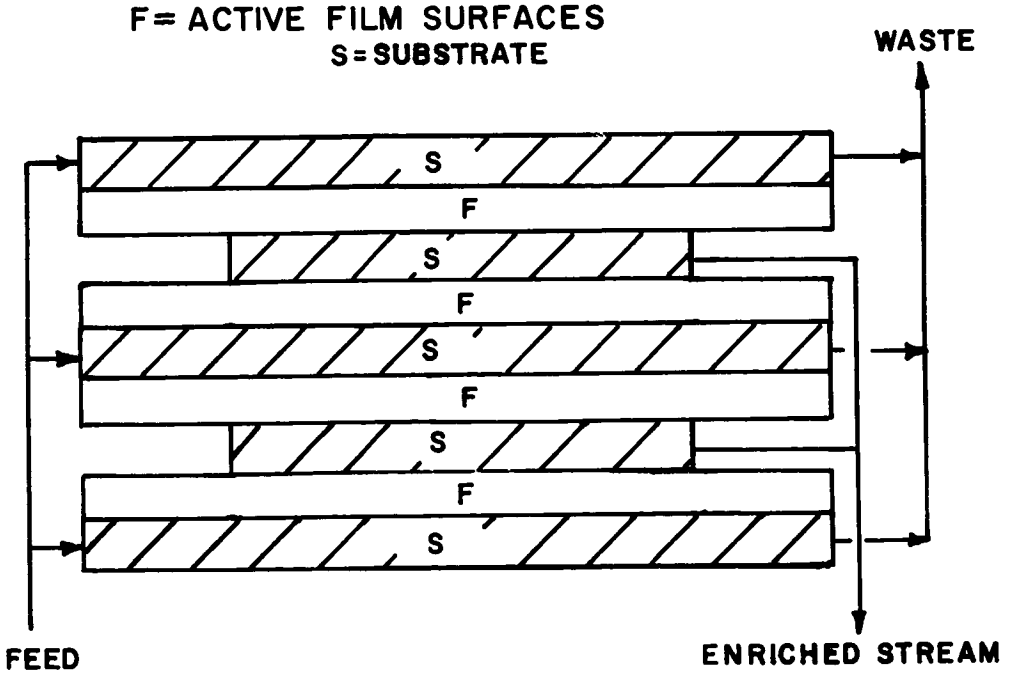

FIGURE 3
SECTIONAL VIEW OF POTTED CELL

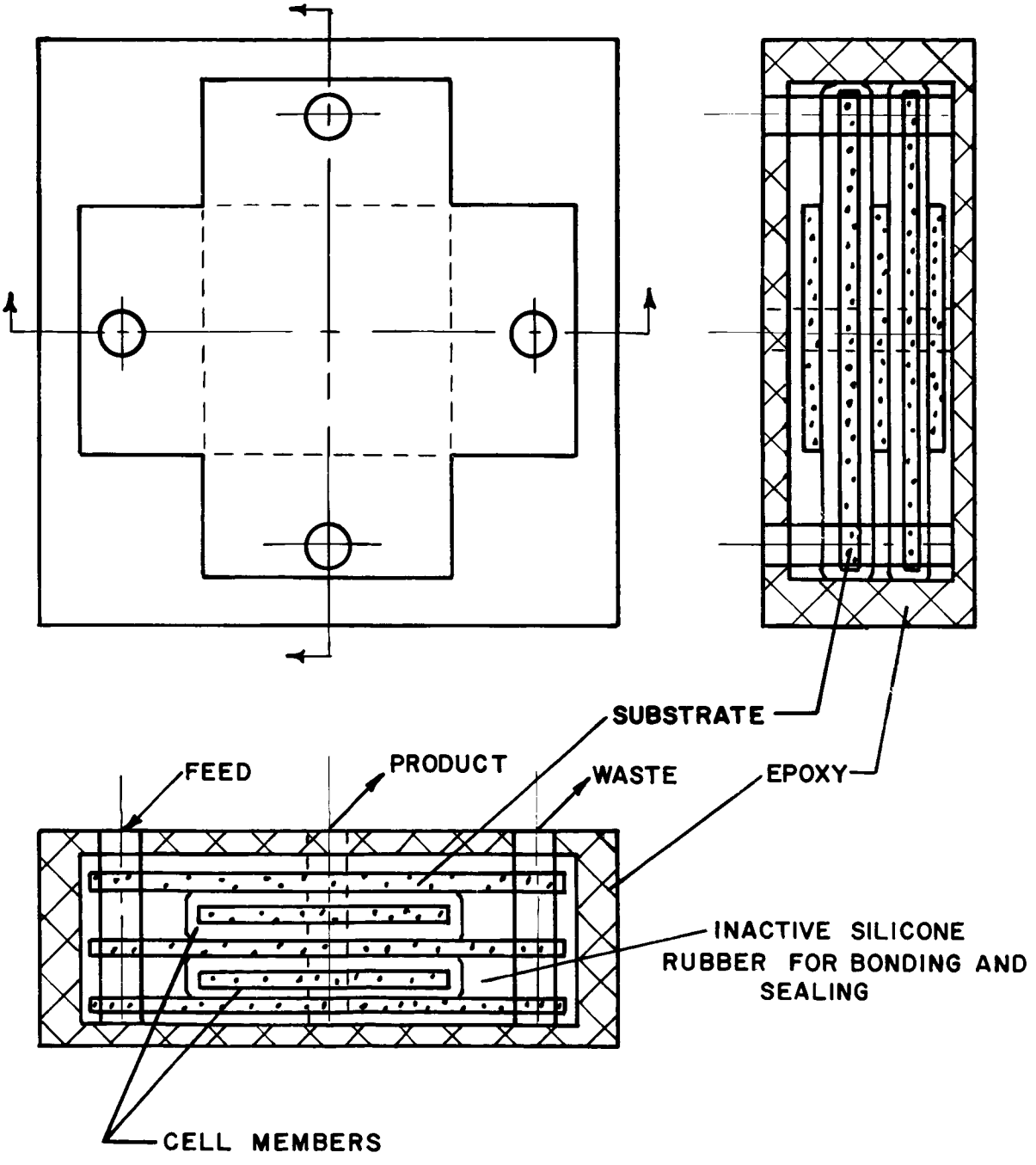

application of permeability separations to space craft use is severly limited.

The proposed design presents a unique solution to this area-volume problem. The design is basically very simple. It involves the use of a large number of individual separation units connected in parallel. The structure of the cell assembly is such that it permits the interconnections between the individual units to be made without a complicated external piping system. Thus the total volume of the assembly is considerably reduced. Figures 2 and 3 are schematic representations of the proposed cell assembly. They show that the assembly has a multilayered structure. Each layer of the assembly is a small separation unit capable of producing some part of the total separation. This basic unit of the cell assembly consists of three substrates and two silicone rubber films. Figure 4. It is assembled by placing one of the substrates between the films. The edges of the film are then sealed to provide a leak tight enclosure. Thus if the films are consistant, gases can reach the enclosed substrate only by permeating through the film. The two remaining substrates are centered at right angles and on opposite sides of this film envelope, thereby forming a "Greek cross" configuration. These two substrates act as channels for

FIGURE 4
STRUCTURE OF CELL MEMBER
AND
CELL ASSEMBLY

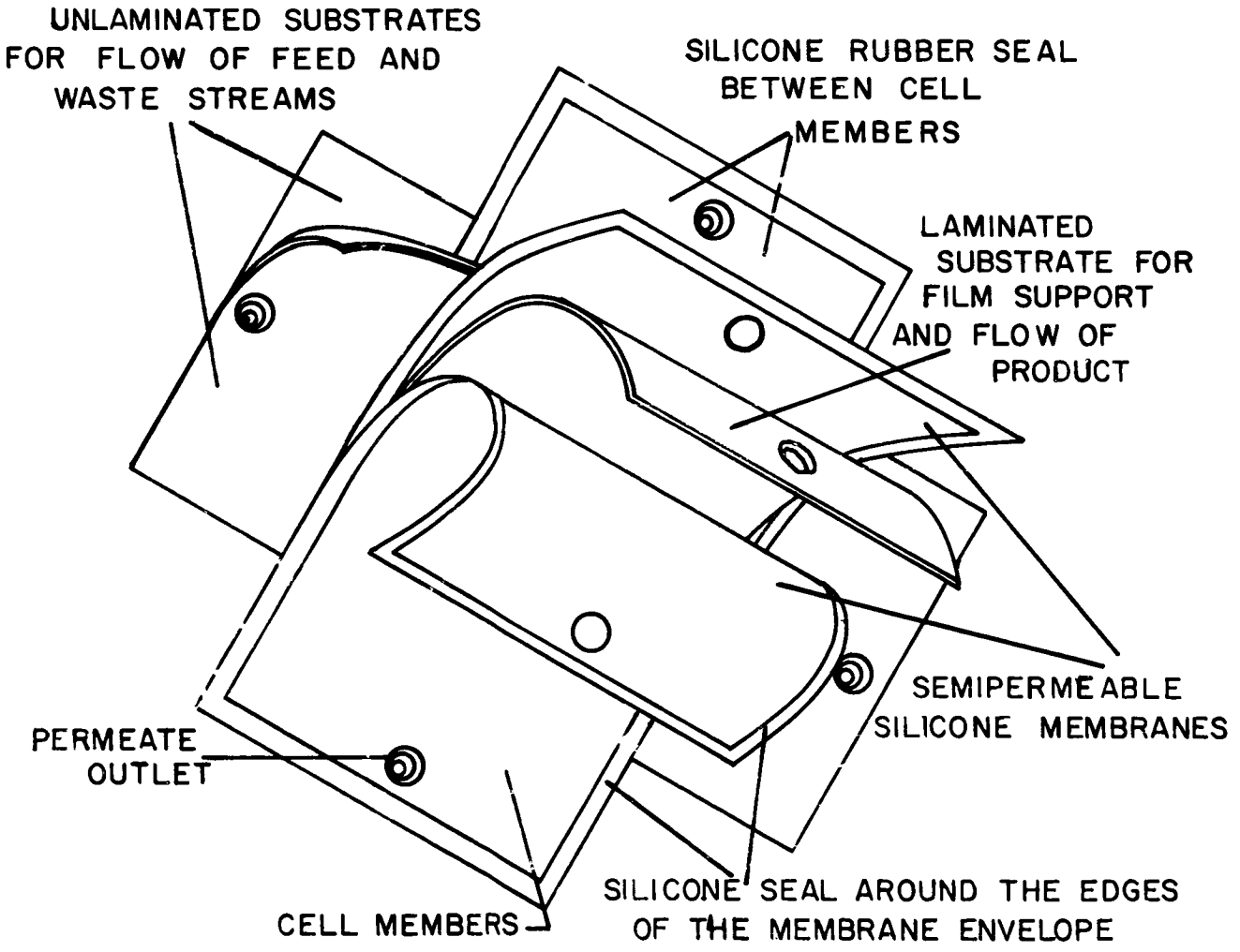

bringing the feed stream into contact with the film surfaces and for removing the unpermeated waste gases from them. The substrate enclosed within the silicone films serves two purposes. It supports the films, thereby helping to relieve the pressure stresses place across them, and it also acts as a channel through which the enriched gases can be removed after they have permeated the film.

The cell assembly is constructed by stacking these individual units on top of one another until the desired size is obtained. The Greek cross shape which the completed assembly assumes was designed by Dr. Major to facilitate the admittance and withdrawal of the various gas streams. As pictured in the drawings, the connections between the unit layers are made by boring holes through them at the extremities of the arms of the cross. In this location there is very little possibility of damaging the selective membranes during this "tapping" operation.

As a final construction step, the assembly is potted in an epoxy resin. This technique helps to prevent the occurrence of leaks and ruptures which may result from sudden pressure changes or other accidental abuse during the operation of the assembly.

Cell Operation

The theory for calculating the enrichment of a binary mixture has been well developed by Weller and Steiner (12) (13) for the single stage permeability operation. The Weller Steiner Case I for perfect mixing of the gases on both sides of the film was chosen to describe the proposed permeability cell. Using this model it is assumed that the effective composition on the high pressure side of the selective membrane will be equal to the composition of the gas leaving that region. Correspondingly, the composition on the low pressure side of the membrane will be the same as the gas stream leaving that region.

Based on the above assumption and on Fick's law of diffusion, Kammermeyer and Brubaker (2) derived equations for binary, ternary, and quaternary systems. The following equation represents the equilibrium dynamics for the binary system:

$$\frac{(X_p)}{(1 - X_p)} = \alpha \frac{(PX_o - PX_p)}{(P(1 - X_o) - P(1 - X_p))} \quad (1)$$

where (X_p) is mole fraction of component A in the product stream.

$(1-X_p)$ is mole fraction of component B in the product stream.

(X_o) is mole fraction of component A in the waste stream.

$(1-X_o)$ is mole fraction of component B in the waste stream.

α is the ratio of the pure gas permeability coefficients for gases A and B. (Separation factor) = $(\overline{PA}/\overline{PB})$

P' is the total pressure on the high pressure side of the membrane in cmHg.

P is the total pressure on the low pressure side of the membrane in cmHg.

Equation (1) is a quadratic equation in terms of (X_p), and a solution for (X_p) can be written in the form:

$$(X_p) = \frac{-b + \sqrt{b^2 - 4ac}}{2a} \qquad (2)$$

The values of the quantities a, b, and c were obtained using overall material and component balances. Based on (θ) the cut, and (X_F) the mole fraction of (A) in the feed stream, the following values were obtained:

$$a = (\alpha - 1)(P + \theta\Delta P)$$

$$b = -(\alpha - 1)(\theta X_F + \theta\Delta P) - \Delta P - \alpha P$$

$$c = \alpha X_F$$

where θ = cut = $\frac{\text{Product rate (cc/min)}}{\text{Feed rate (cc/min)}} = \left\{1 - \frac{\text{Waste rate}}{\text{Feed rate}}\right\}$

$\Delta P = (P' - P)$ cmHg

X_F = mole fraction of component A in the feed stream.

Typical separation curves derived from this theoretical equation are plotted in Figure 11 of the Appendix.

It is of interest to note that for a permeability separation of a binary mixture, the degree of separation

with respect to product purity will approach a maximum value as the amount of product removed approaches zero. Theoretically this implies that the composition of Component A in the waste stream, (X_o), approaches the composition of A in the feed stream, (X_F), as the composition of A in the product, (X_p), approaches a maximum. Moreover, the pressure on the product side of the membrane recedes to zero. Under these conditions equation (1) reduces to:

$$X_o \longrightarrow X_F, \quad P \longrightarrow 0, \text{ and } X_p \longrightarrow X_p(\max)$$

$$\frac{X_p(\max)}{(1 - X_p)\,(\max)} = \frac{\alpha X_F}{(1 - X_F)} \qquad (3)$$

Although these conditions produce the highest degree of product purity for the single stage operation, they will not produce the greatest amount of product take off and overall separation. Therefore a system is seldom operated for these conditions.

Furthermore, the fact that the purity of the product does approach a finite maximum, or upper limiting value, is evidence that a permeability separation can not produce a complete separation in a single pass. This can be accomplished only with a membrane having an infinite separation factor ($\alpha = \infty$). Unfortunately at the present time there is no known membrane having a

separation factor greater than 10 for a mixture of carbon dioxide and oxygen. A large number of membranes have separation factors of less than 10 for this mixture, however, and these offer the possibility or very nearly complete separations when employed in cascade arrangements.

In those instances when X_F becomes quite small the quantity $(1 - X_F)$ will be approximately equal to unity. Under these conditions equation (3) may be further reduced to

$$X_p(\max) = \frac{\alpha X_F}{1 + \alpha X_F} \qquad (4)$$

DESCRIPTION OF APPARATUS

Introduction

This investigation consisted of three distinct phases. The first phase involved an investigation of the materials and techniques needed for the construction of a permeability cell. The second phase revolved around the construction of a prototype of the cell. The third and final phase dealt with tests to determine the operating characteristics of this prototype. Each phase of the investigation required a number of different apparatus arrangements. Many of these apparatus arrangements have already been described in previous progress reports. For this reason, the following discussion will contain only brief summaries of these particular arrangements, as well as references to more complete discussions of them.

Film Preparation and Testing (20) (22)*

Silicone rubber samples were mixed according to the instructions recommended by their respective manufacturers, Dow Corning and General Electric. A Gardner precision drawing knife, which could be adjusted to produce films with thicknesses of from 5 to 20 mils, was used to create films on clean plate glass. For this operation it was essential for the glass to be completely free of

* These numbers refer to references listed in the bibliography which give a more complete description of the subject.

FIGURE 5
SCHEMATIC
COMPACT GAS-PERMEABILITY APPARATUS
C.J.M.

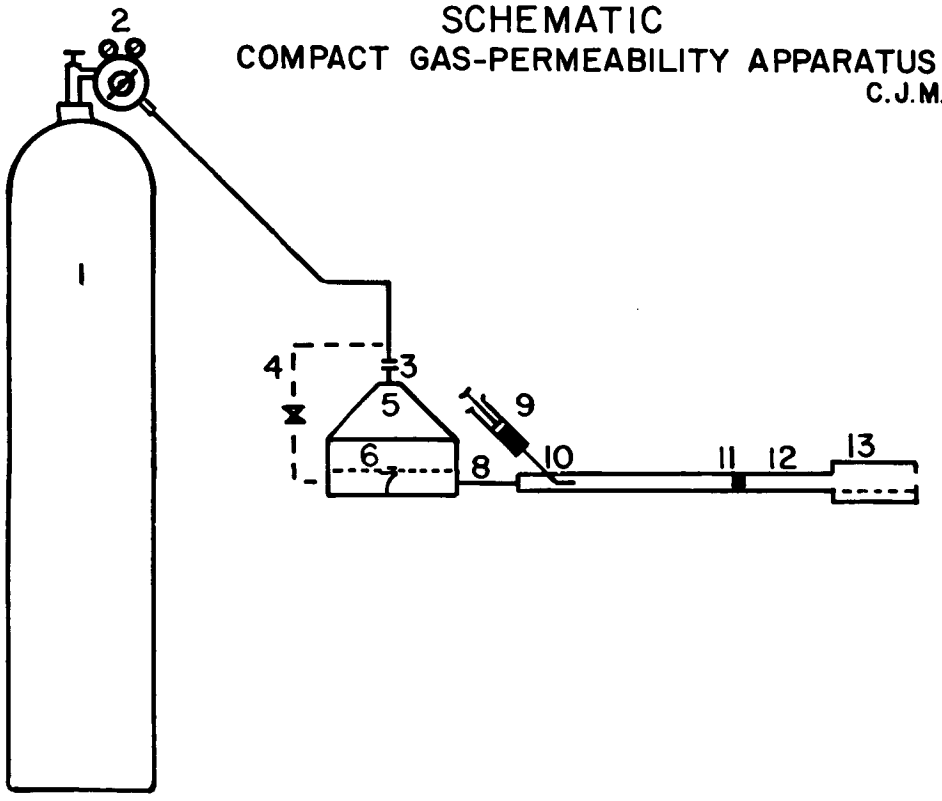

scratches and dust particles in order to insure continuity of the film and to facillitate its removal after polymerization.

The selective properties of the silicone films were tested with a compact gas-permeability apparatus designed and produced by the C. J. Major Co. (5). A schematic representation of the apparatus is depicted in Figure 5. The unit has a durable construction, is completely portable, and does not require a vacuum source, utilities, or special tools for assembling and disassembling. The permeability coefficient of the film being tested is determined by timing the displacement of a water slug along a colibrated capillary tube. Results obtained with this apparatus correlated well with those of larger and more elaborate arrangements.

A significant amount of permeability data covering a wide range of different polymers and several gases had been accumulated by Major, Kammermeyer, Roberts and McIntosh (6) (8) (7) (11) prior to this investigation. Major and McIntosh also extended the permeability data for several silicone rubbers over a temperature range of 40°C to 10°C. (20) (8). All of these sources were useful in the final analysis and selection of the cell membrane.

FIGURE 6
SCHEMATIC
SUBSTRATE POROSITY APPARATUS

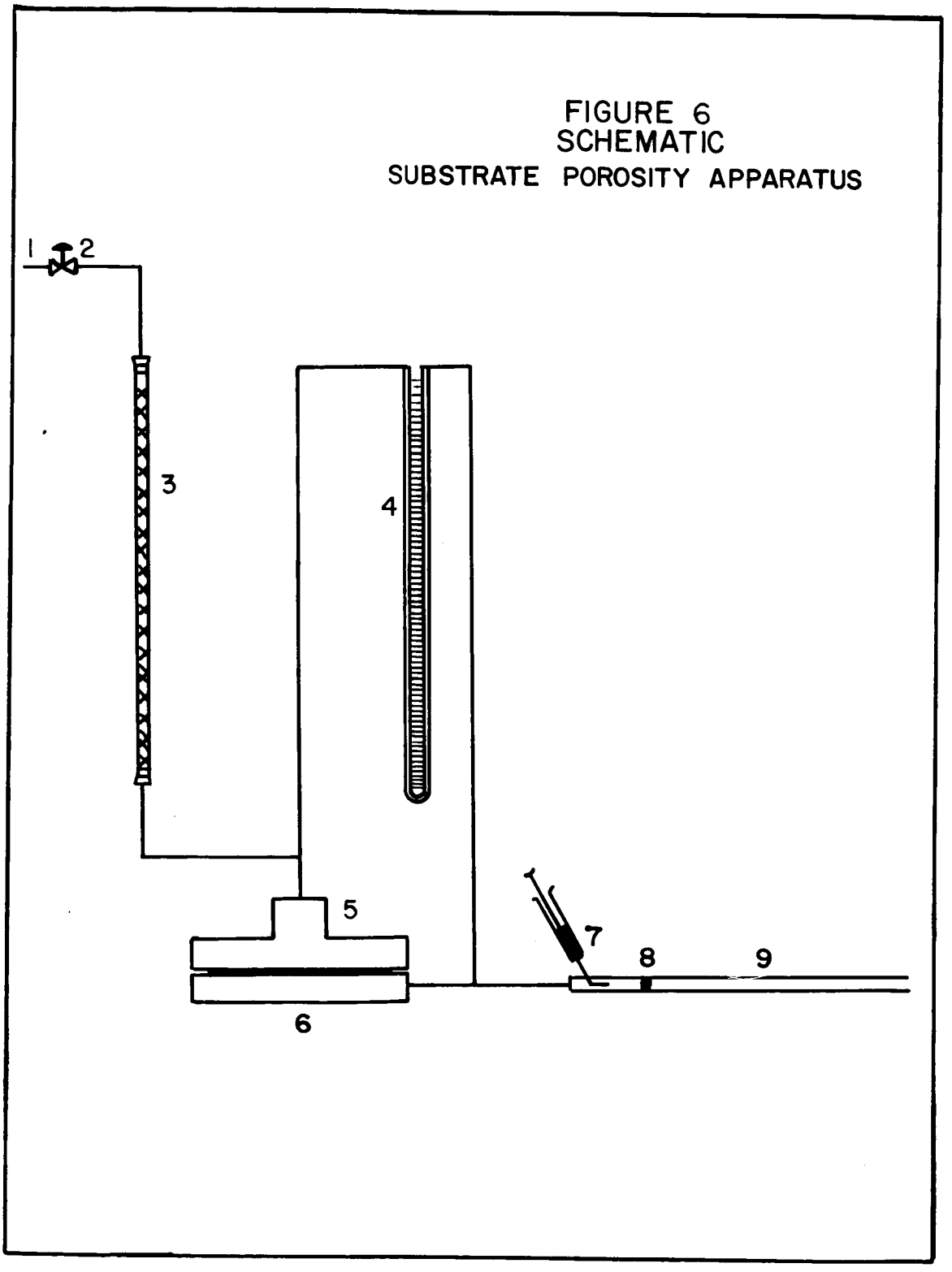

Substrate Testing (15) (20) (16) (22)

A preliminary study of the structure of the proposed permeability cell revealed the need for a substrate which would separate and support the semi-permeable films. In addition these substrates were to provide channels through which the gases could travel in going to and from the film surfaces. Since it was desirable that these substrates offer a minimum of resistance to the gas flow, the porosity of a material became the primary criterion for judging its excellence as a substrate. An indication of the porosity of potential substrate materials was obtained with the apparatus depicted in Figures 6 and 7.

This apparatus was designed to measure the volumetric flow rate of air edgewise through the plane of the sample. As shown by the schematic diagram, this was accomplished by measuring the rate of slug travel through a capillary tube in a manner similar to that for the compact permeability apparatus.

Figure 7 depicts an exploded view of the unit for holding a sample of the substrate materials. The body of the assembly is constructed of machined Lucite, and the separate halves are held together by a bolt through each of the four corners. Air enters and leaves the cell through 1/4 inch flare couplings. The substrate

FIGURE 7

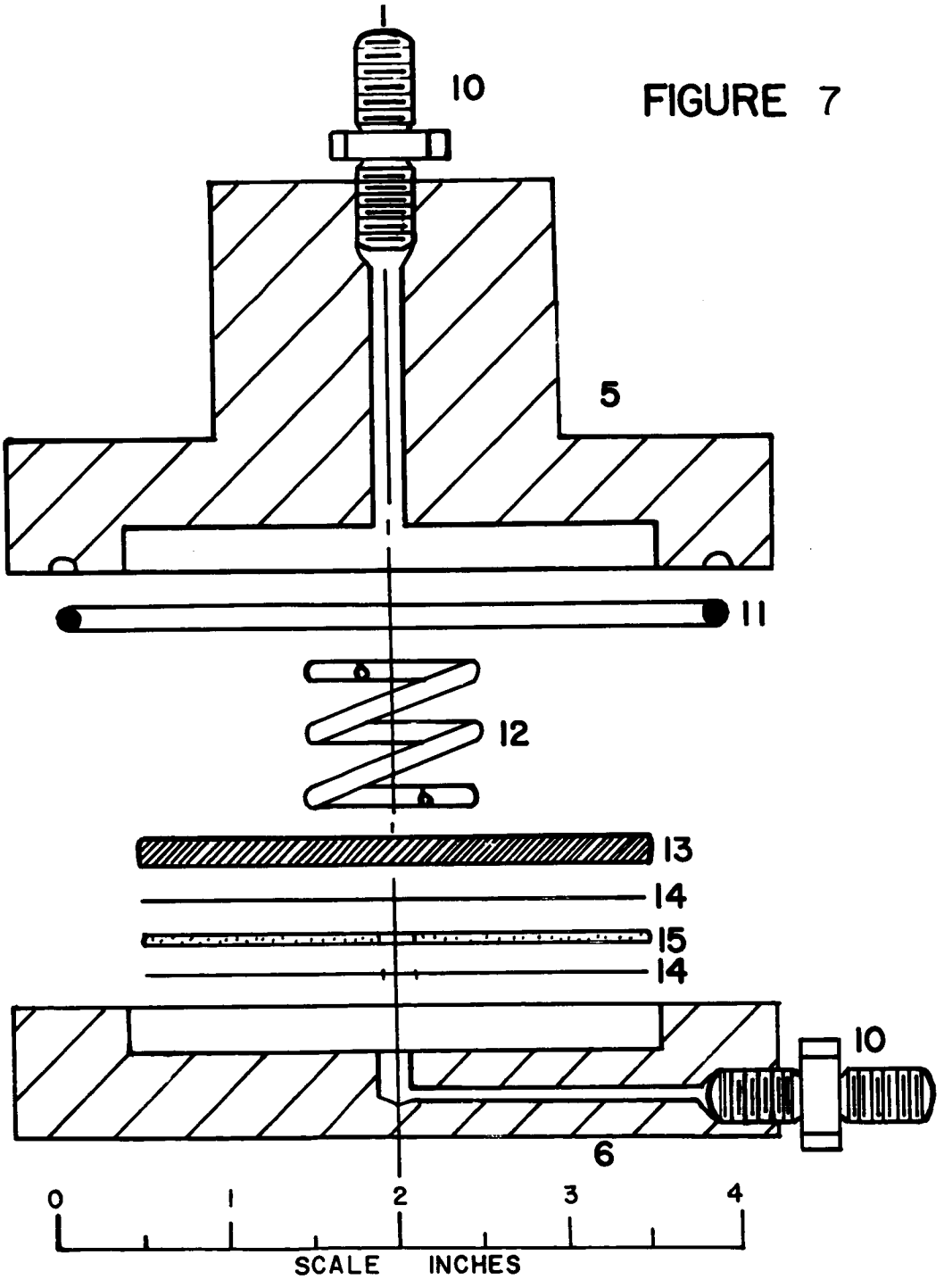

SUBSTRATE SAMPLE HOLDER

material is held in place by pressure exerted by compression of a spring. Air is forced to flow radially from the periphery of the sample to its center by the bottom portion of the cell and a machined aluminum disk resting on top of the sample. As an added precaution, silicone films were placed above and below the substrate sample. These films acted as gaskets and minimized gas flow by channeling across the samples surface. Thus a better picture of the materials actual porosity was obtained.

Cell Testing (23) (24) (25)

Prototypes of the permeability cell were tested to determine their ability to effect a separation and to measure their handling capacity. Figure 8, page 23 is a schematic representation of the apparatus used for testing the separation produced by a cell.

A gas proportioning valve ($\overline{15}$)* designed by Dr. Major was used to produce a continuous flow of a constant gas mixture. This instrument has excellent application over the small carbon dioxide concentration ranges used in the test.

A Fisher Porter ($\overline{12}$) and a Roger Gilmont ($\overline{9}$) rotameter were used to measure the flow rates of the

* These numbers, ($\overline{15}$), with the superscripted bar refer to equipment numbers on apparatus figures.

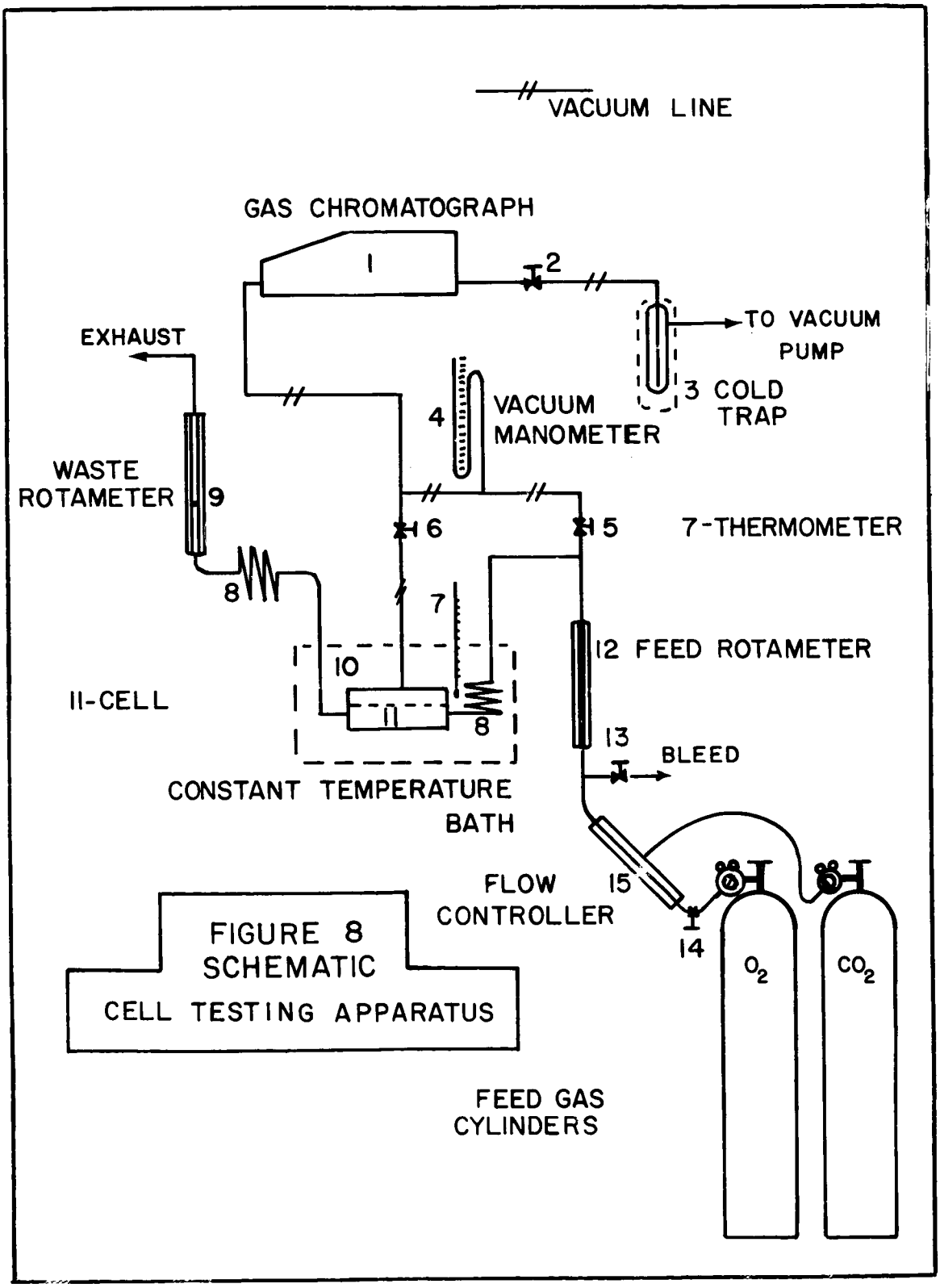

FIGURE 8
SCHEMATIC
CELL TESTING APPARATUS

feed and waste streams. Their capacities ranged from 0 to 260 std. cc of air per minute.

The driving force across the cell membranes was produced by creating a vacuum on the product side. A Welch Duo-Seal vacuum pump was used for this operation. A cold trap for volatile collection was used as recommended in connection with the operation of the pump. (3)

Analysis of the feed and product streams was accomplished using a special vacuum setup on a Beckman GC-2 gas chromatograph (1). A 4-foot silica-gel column was used to effect a partition of the sample within the instrument. A closed end Fisher manometer (4) was used to record the pressure on the product side of the membranes. This manometer also served to record sample sizes, and thereby provided uniform sampling in connection in the chromatographic analyzer.

A Sargent Thermometer, Model S. W., temperature control bath (10) was used to maintain a constant temperature during each run. This unit has its cooling, heating, and agitation systems all integrated into a single control panel. When properly adjusted it maintained a temperature to within + 0.01°C. Temperature readings were taken with a Fisher thermometer (7) having a range of -36° to 54°C, and divisions of 0.2°C.

Copper tubing (1/4 inch O.D.) and sweat fittings

were used for all lines subjected to vacuum pressures. Copper conditioning coils (8) were also employed to help bring the gas streams to equilibrium upon entering and leaving the bath portion of the system. Tygon tubing (3/16 inch O. D.) was used to make all the remaining connections within the system. Vacuum grease was used to help seal these connections.

To check the capacity of the substrates within the cell, a simple setup using a mercury manometer and a wet test meter were used. See Figure 17. (26)

EXPERIMENTAL PROCEDURE

Permeabilities of Silicone Rubber Films (6) (8)

All of the silicone rubber samples were prepared according to the instructions of their respective manufacturers. Membranes were made by drawing the unpolymerized samples out into films of the desired thickness on clean plate glass. A period of 12 to 48 hours was required for these films polymerize. When cured they were peeled from the glass and cut to the proper size required for testing in the compact gas permeability apparatus.

To make a permeability measurement, the sample to be tested was inserted into the film holding portion of the apparatus. After the film holder had been reassembled, it was connected to the test gas cylinder by means of a quick disconnect coupling. Next the test gas was released from the cylinder and regulated to the desired pressure. By means of a bypass connection, the downstream side of the film was purged several times with the test gas. A small slug of water was then injected into the capillary tubing and readings were taken of the slug position at regular intervals. Table 4 depicts the data obtained for a typical run with this apparatus.

Substrate Porosities (6) (8)

The procedure for testing substrate materials is essentially the same as that which was just described for testing films. Here again the sample material was first cut to size. This particular apparatus, Figure 7, required a disc shape having a diameter of three inches and a 1/4 inch hole through its center. The sample was inserted into the holder and secured for testing. All the porosity tests were conducted with compressed air so there was no need for purging the system, and air was admitted directly into the unit after passing through a drying tube. A slug of water was injected into the capillary tube, and readings were taken of its position at regular intervals. The pressure drop across the specimen and its thickness were also recorded for each sample. Both laminated and unlaminated substrates were tested with this apparatus. The data taken during a typical run is presented in Table 5.

Laminating

The laminated substrates were prepared by a technique whereby the fresh film was allowed to partially polymerize before application of the substrate. This technique was developed to keep the uncured film from soaking into the substrate, thereby destroying both the porosity of the substrate and its own continuity. The time

required for this partial polymerization to occur was dependent upon the temperature of the room and the amount of catalyst added. After a sufficient amount of practice, however, it was possible to determine the proper application time by testing the tackiness of the film with one's finger tip.

Cell Construction (21) (23) (24) (27)

As was previously mentioned, the permeability cell is actually a multilayer assembly with each layer performing as a separation unit which contributes in some degree to the overall total separation. Each layer is made up of a "cell member" and two substrates placed at right angles to the cell member.

Since the "cell member" performs the separation within each layer, it is the most fundamental part of the assembly. Each cell member consists of a single substrated laminated with silicone film on all of its external surfaces. The procedure for construction was as follows:

(1) Substrates were cut into rectangular shapes having the dimensions 2 1/2 in. by 3 1/2 in. These were laminated to silicone films.

(2) When the films had cured, they were trimmed so that only 1/8 inch of unlaminated film remained along the edge of the substrate.

(3) These laminated substrates were examined by eye for discontinuities in their film surfaces. Those having no apparent flaws were separated and used in the following step.

(4) Films were prepared, and the unlaminated surface of the substrate was laminated. After curing the excess film is again trimmed off.

During this last step the purpose of the 1/8 inch of silicone fringe retained from the first lamination becomes apparent. This portion of the first film bonds directly to the tacky surface of the second, which seals the edges of the substrate, completely encasing it in an "envelope" of silicone film. Thus if both the films remain continuous, gas can reach the enclosed substrate only by permeating through the film.

When a sufficient number of cell members had been constructed, the cell was assembled by alternately stacking at right angles a substrate, cell member, substrate, cell member, substrate, ...etc., until the desired number of layers had been reached. For this investigation the number of layers used ranged from 3 to 15. In the process of stacking the individual layers, the extremities of the cell members were bonded to one another by the application of fresh silicone to

their surfaces. Upon polymerization this produced a continuous medium through which the top holes could be bored to connect the cell members. This bond was quite necessary for preventing cross leakage within the cell.

As a final step the crude assembly was given another thin coat of silicone rubber over the entirety of its exposed surface. This final coat was to prevent the epoxy potting compound, used in the finishing stages, from penetrating the porous substrates and ruining them.

The potting operation using Armstrong C-4 epoxy resin with Activator W was carried out in a precast silicone rubber mold. Since the resin was quite fluid in its unpolymemerized state, the cell assembly was merely centered in the mold and the epoxy allowed to flow around it. The curing time for the epoxy was roughly 24 hours. By using a microwave generating source this time could be reduced to 3 to 4 hours. However, since the microwave antenna was circular and the assembly rectangular, curing by this method was often uneven and air was frequently trapped beneath the assembly.

After the epoxy had cured, the tap holes were drilled at the extremities of the arms of the assembly. Sections of 1/4 inch O. D. copper tubing were sealed in the holes with fresh epoxy resin. Connection could then be made to the copper tubes whenever it was desired to

do so.

Testing the Cell

Using the apparatus shown in Figure 8, a typical run began by bringing the temperature bath and the gas chromatograph to equilibrium. Under the best conditions this usually required from two to three hours. Once stabilization was established valves (5) (6) and (13) were closed and valve (2) opened. This procedure exposed the sampling portion of the system to the vacuum source, thereby removing any gaseous contaminants present in this portion of the system.

While this evacuation of the low pressure side was taking place, the flow of feed gas was started. The desired feed composition was approximated by first opening the valves on the oxygen cylinder. Using the flow control valve (14) the oxygen rate was regulated to the desired rate as indicated by the rotameter reading (12). Knowing the flow rate of the pure oxygen, the carbon dioxide regulator was set to produce just enough flow of CO_2 to give the correct feed composition. Under these conditions both rotameters indicated that feed gas was flowing through the cell.

With the feed gas mixture flowing, valve (2) to the vacuum was closed and valve (5) opened long enough

to permit a sample of the feed to enter the gas chromatograph (1). The size of the sample taken was measured with the closed-end manometer (4). Once the sample had been analyzed, valve (2) was reopened. When the manometer again registered complete evacuation, another sample of the feed was taken in the manner just previously described. This sampling procedure was continued until a constant feed composition was obtained as indicated by peaks of equivalent height on the chromatographic recorder for consecutive samples. If this composition was not that which was desired, adjustment was made by regulating the oxygen flow rate through the flow control valve (14). Usually the desired feed composition was obtained with 4 to 6 samplings.

Once the feed composition had been determined, valve (6) was opened. This exposed the product side of the cell membranes to the vacuum source and initiated the separation process. Valve (2) was then partially closed to throttle the vacuum and thereby create the desired sample pressure on the vacuum side of the cell. Under these conditions the system was then permitted to come to equilibrium. Several trial runs indicated that this equilibrium could be reached in a minimum period of 15 to 20 minutes.

Once equilibrium had been established, the rotameters,

thermometer, and barometer were read and their readings recorded. The pressure in the product stream was read on the closed and monometer and also recorded. A sample of the permeated gas was then introduced into the chromatograph for analysis. The peak heights which appeared on the recorder were identified, and the corresponding compositions which they represented were computed. This completed the data taking required to determine this one point for the run.

To obtain another point valve 2 was reopened completely to again evacuate the product side of the system. While the evacuation was taking place, valve ($\overline{13}$) was opened very slightly to permit a small amount of the feed gas to bleed out into the atmosphere. This had the effect of establishing a new cut for the next data point, since a constant product rate is being drawn off while the feed rate to the cell has now been slightly decreased.

The procedure just outlined for taking the first data point of the run was followed for the second and each succeeding point until the complete range of possible cuts had been covered. After the last point had been obtained, the feed composition was checked again before proceeding to new operating conditions. Data from a typical run is shown in Table 6.

Substrate Capacity of Cell Assembly (12)

The capacity of the unlaminated substrates within the cell assembly was measured with the apparatus shown in Figure 15. As shown by the diagram an air source with a control valve was attached to one of the copper leads of the cell. The corresponding lead leaving the cell was connected to a precision wet test meter. A mercury monometer was installed between these two leads as shown in the diagram. Using this arrangement, the pressure drop across the cell could be recorded for each flow rate measured with the test meter. Data from several runs is plotted in Figure 17. The flow rates have all been normalized.

DISCUSSION OF RESULTS

Cell Membranes

Prior to this investigation, Major et al (6), (11) had reported a significant amount of permeability data for a large number of different membranes and gases. Based upon the results of this work and data obtained in literature searches, it was decided that silicone rubber membranes would be used in the construction of the proposed cell.

Nine different formulations of these silicone elastomers were obtained from their respective manufacturer, Dow Corning or General Electric. They were cast into films and their permeabilities to the pure gases carbon dioxide, oxygen, and nitrogen, were measured over a temperature range of 5°--45°C. As had been predicted by the literature, this type of elastomer demonstrated a relatively high rate of permeation and good selective properties for carbon dioxide as opposed to oxygen. The results of the tests may be found in Table 1. From these data it is apparent that each type of elastomer exhibited approximately the same 5 to 1 ratio between the carbon dioxide and the oxygen permeability coefficients at room temperature. The carbon dioxide to nitrogen ratio is about 9 to 1 for the same temperature Actual

PERMEABILITY COEFICIENTS - SILICONE RUBBER

TABLE I

Silicone Rubber Membrane	T(°C)	Permeability Constant $\bar{P}$ $\frac{Cm^3(STP)Cm.x10^9}{Sec.Cm^2Cm.Hg}$			Separation Factor	
		CO_2	O_2	N_2	αCO_2-O_2	αCO_2N_2
RTV-501	23.0	285	53.8	25.8	5.30	11.05
	32.5	278	59 3	29.2	4.69	9.52
	43.0	280	65.7	33.4	4.26	8.38
	6.0	270	42.5	18.8	6.35	14.36
RTV-502	23.0	286	55.3	26.3	5.17	10.87
	33.0	280	60.4	29.9	4.64	9.36
	43.0	282	66.3	34.1	4.25	8.27
	10.5	269	45.9	20.7	5.86	13.00
RTV-40	24.0	205	42.6	21.4	4.81	9.58
	33.5	203	45.8	23.3	4.43	8.71
	43.0	197	46.8	24.1	4.21	8.17
RTV-11	29.0	240	50.6	24.6	4.74	9.76
	33.0	238	51.4	25.5	4.63	9.33
	43.5	235	57.1	29.0	4.12	8.10
RTV-601	33.0	286	75.6	45.0	3.78	6.36
	43.0	282	77.7	47.5	3.63	5.94
RTV-20	28.5	191	39.9	18.8	4.79	10.16
	33.0	190	41.0	19.8	4.63	9.60
	43.0	189	45.6	25.2	4.14	7.50
Eccosil 4712	20.5	137	28.0	13.0	4.89	10.54
	32.0	138	31.2	15.2	4.42	9.08
	43.5	139	34.3	17.4	4.05	7.98
Sylgard 182	20.5	204	40.0	18.1	5.10	11.27
	33.5	206	46.1	21.7	4.47	9.49
	43.5	205	51.2	24.9	4.00	8.23

permeability values for carbon dioxide range between 140×10^{-9} and 300×10^{-9} while those for oxygen range between 30×10^{-9} and 80×10^{-9}.

Figures 9 and 10 show plots of the permeability coefficient vs. ($1000/T^{\circ}K$) for the silicone rubbers RTV-501 and RTV-502 with respect to the pure gases, oxygen, nitrogen, and carbon dioxide. From these plots it is apparent that the permeability coefficients for these elastomers with respect to carbon dioxide is independent of temperature. Permeabilities obtained for oxygen and nitrogen do, however, show a direct dependence upon temperature. Since the oxygen permeability coefficient decreases with temperature while the carbon dioxide coefficient remains constant, their ratio ($\bar{P}CO_2/\bar{P}O_2$) must increase with decreasing temperature. These data would then seem to indicate that the optimum operating conditions for a completed cell is somewhere in the lower temperature ranges where the separation factor is the greatest.

With but two exceptions, the permeability data obtained is essentially the same for all the silicone rubber formulations which were tested. However, RTV-501 silicone rubber, manufactured by Dow Corning, was selected for use in cell construction. This selection was based primarily on its excellent workability in all

FIGURE 9

PERMEABILITY OF RTV-501 SILICONE RUBBER

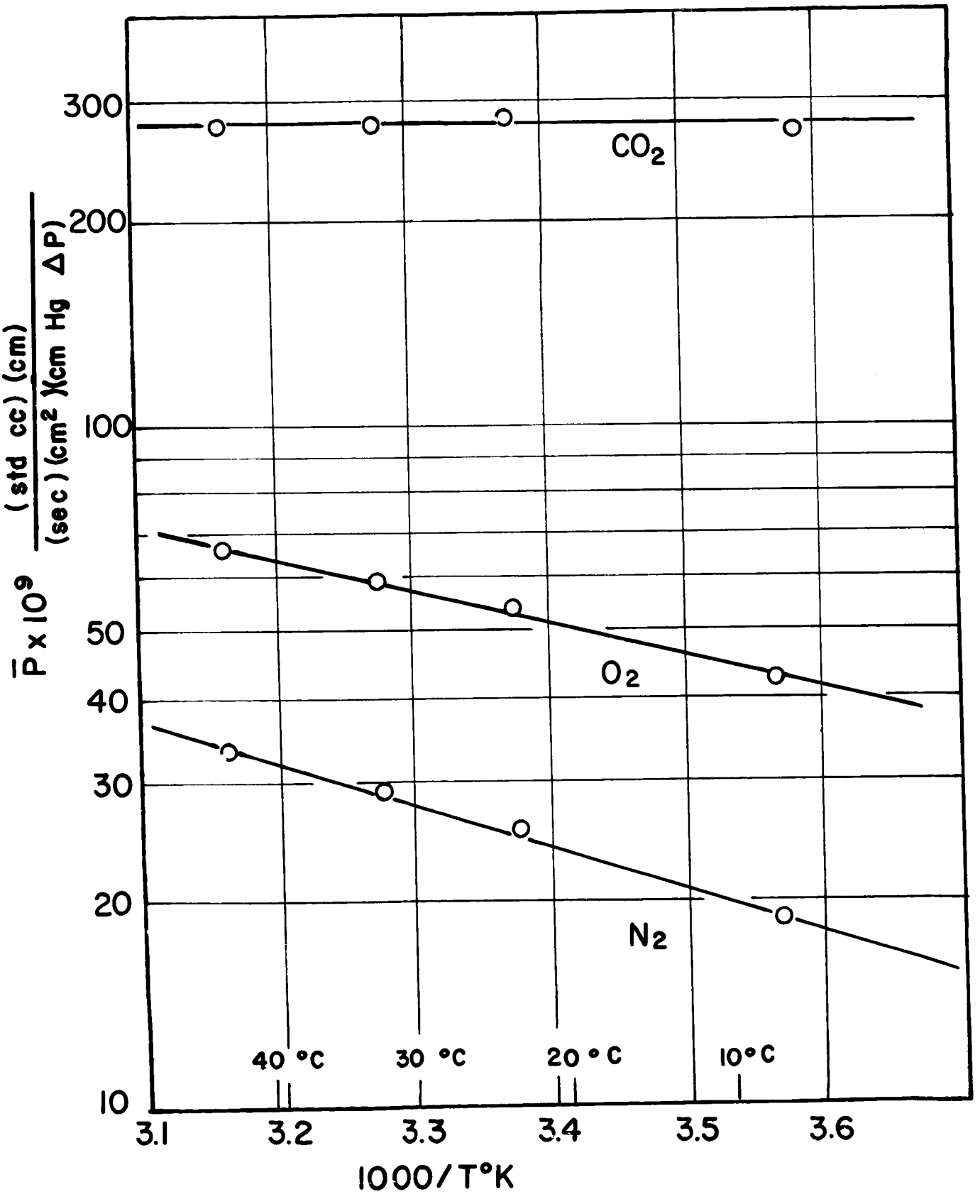

FIGURE 10

PERMEABILITY OF RTV-502 SILICONE RUBBER

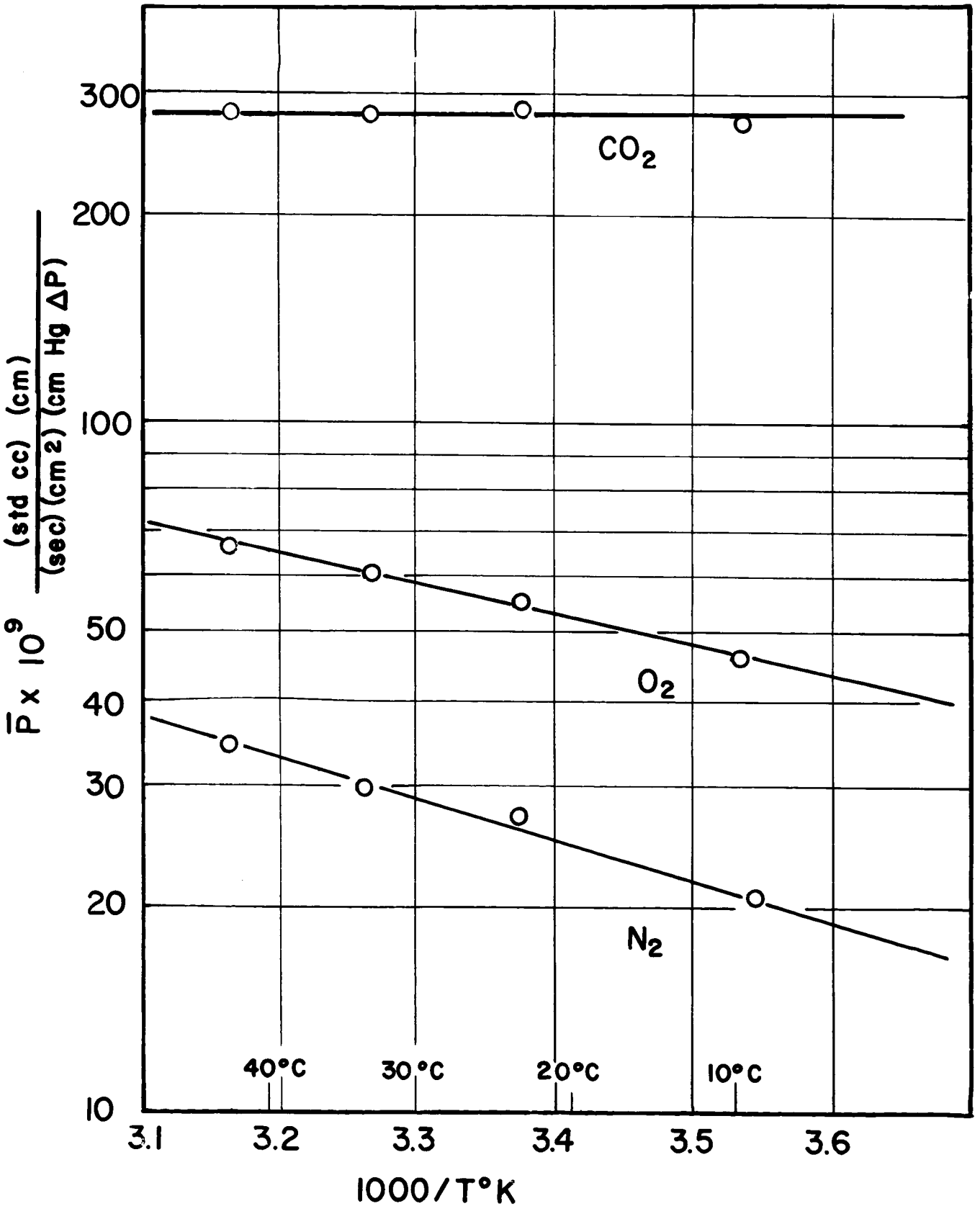

phases and its superior film quality in the polymerized phase.

Substrates and Porosity

Lined notebook paper, filter, paper, Nibroc paper towel, kraft paper, Gelman Polypore, and typing paper were the materials selected for testing as potential substrates. The volumetric flow rate of air through the plane of each sample was measured. These rates were then normalized to give a porosity value which was independent of the specimen's geometry. Since a relative porosity was desired for each sample, lined notebook paper was taken as the standard, and its porosity reading was set equal to unity. Based upon this standard, filter paper exhibited the highest porosity of the samples tested and typing paper the lowest. Table 2 shows the relative porosity values for each of the samples tested. Porosity values larger than any of those shown in the table were measured for samples of toilet tissue and nylon stocking. However, these materials were not seriously considered as potential construction materials because they were too thin, flimsy, and generally difficult to work with.

An attempt was also made to correlate the surface texture of a sample with its porosity value. As expected

TABLE 2

Substrate Porosity

Sample	Relative Porosity	Texture
Lined paper	1.00	Glossy
Filter paper	11.80	Wrinkled, Coarse
Paper towel	8.70	Coarse
Kraft paper	5.90	Rough
Gelman Polypore	4.40	Tight Woven Cloth
Typing paper	0.46	Smooth, Tight

TABLE 3

Laminated Substrate Porosity

Sample	Relative Laminated	Porosity Unlaminated
Lined paper		1.00
Paper towel	5.95	8.70
Kraft towel	2.36	5.90

penetrated. Since a substrate was desired which would least restrict the flow of gases, the effects of any channeling which might occur were considered somewhat desirable. Excessive penetration of the substrate by the silicone was, on the other hand, considered most undesirable and to be avoided.

Since the Nibroc paper towel had a relatively high porosity and seemed to laminate well to the silicone films, it was selected for use as a substrate in the construction of the cell.

Cell Assemblies

Nearly 30 prototypes of the proposed permeability cell were constructed and tested. Approximately one-fifth of these effected a satisfactory separation while the remaining four-fifths were not successful. For this investigation a cell producing a satisfactory separation was defined as one having a carbon dioxide to oxygen ratio greater than 4.8 for its separation factor ( ). A large portion of the cells which were rejected on this basis had separation factors ranging from 4.5 down to 2.0.

The results of the tests performed on a satisfactory cell, 3A, are depicted graphically in Figures 11 to 13 in the Appendix and in tabular form in Tables 6 to 14. Figures 11 to 13 depict the separation curves for the cell at 3 different temperature isotherms, 40°C, 25°C, and 0°C

samples consisting of large coarse fibers and rough surfaces gave the best porosity readings, while those with tight glossy textures gave the poorest. Table 2 also gives the textures which were assigned to each of the samples tested.

Of the materials tested, Nibroc paper towel and kraft paper were selected for further study and testing. This selection was based on their high relative porosity, availability, and workability. Both substrates were laminated to RTV-501 silicone films, and the porosities of these laminated substrates were subsequently measured. The averaged results are tabulated in Table 3, together with their respective porosities for the unlaminated state. The significant decrease in the porosity of a sample after it had been laminated is clearly shown in this table. It was assumed that this porosity decrease was in part an indication that channeling had occurred across the surfaces of the unlaminated sample, and therefore, a true porosity value for flow through the sample had not been obtained. It was also assumed that a portion of the loss in porosity could have arisen from the penetration of the substrate by the tacky silicone rubber during the lamination process. Upon curing it would then effectively plug those porous passages into which it had

and for various feed compositions ranging from 1% to 10% carbon dioxide in oxygen. The curves are plotted as cut (Φ), the ratio of product rate to feed rate, versus the composition of the product stream. The end points of these curves represent the two possible extremes for a separation produced by this cell. When the fraction permeated (cut Φ) is equal to 1.0, there is no separation and the product must of necessity be equal to the feed in both composition and rate of flow. As (Φ) approaches zero the amount of product taken off also approaches zero. At this point the maximum product purity for the separation is achieved. The product composition for this point was predicted from the simplified form of the Weller Steiner Case I equation. It can also be approximated graphically by extropolating the curve to (Φ) equals zero and reading the value of the product composition.

The graph in Figure 14 of the appendix depicts the separation curve derived from the theoretical considerations of the Weller Steiner Case I equation as opposed to that described by the actual data. It is evident from this plot that the Case I equation does not hold for the entire range of (Φ), but begins to deviate at a value of (Φ) between 0.70 and 0.80. This would seem to indicate that perhaps perfect mixing was not occurring

on the high pressure side, and that perhaps the Weller Steiner Case II equation for laminar flow is more applicable for describing the system. The constant temperature runs at 0°C (See Figure 13) with their steep linear slopes do, however, have a closer resemblance to the Case I predictions. It was theorized that this was due to the decreased rate of total permeation at these low temperatures. This would subsequently permit the gases to mix more without being absorbed, which is of course one of the primary conditions which must be met to satisfy Case I.

No conclusive evidence was found to support the theory that better separations are achieved at the lower temperatures. This was thought to be due to a number of reasons. First the concentrations of carbon dioxide were so small in most cases that it was difficult to observe significant changes. Secondly, as pointed out in the above discussion, the mechanism of mixing changes from laminar to turbulent for the low temperature ranges. Since the turbulent mixing is the less efficient of the two mechanisms, the gain produced by the larger separation ratio is immediately cancelled by the switch to turbulence.

Leaks within the assembly were the predominant reason for failure of those cells which did not perform

satisfactorily. For purposes of analysis these leaks were classified either as construction leaks or as membrane leaks.

Construction leaks were those which occurred during some phase of the cell construction. Usually they were created during the cell tapping operation when a barrier bond around a port was accidentally cut or broken. Some leaks of this type were also created when an insufficient amount of silicone rubber was used to seal the tapping regions. These leaks were the easiest to detect, and because they were also relatively large, they often resulted in the complete loss of the cell's ability to effect a separation.

Membrane leaks were almost impossible to detect without making a permeability measurement, and invariably they resulted in only a partial loss of the cell's separation factor. Extremely small inconsistencies in the membrane usually produced this type of leak. These inconsistencies were the result of faulty lamination techniques. For example, if a film was laminated too early while it was still wet, small amounts of the substrate fibers would penetrate the film, and thereby produce small channels along which leaks could develop. However, regardless of the amount of care taken in the preparation of the films or during the lamination

procedure, a few discontinuities will always occur in films having a thickness of 1 to 5 mils. Thus as the area of the films is increased, the probability of a discontinuity occuring and going undetected will also increase. If a film containing one of these discontinuities is subsequently used in a cell assembly, then the cell will not produce a satisfactory separation. Herein then, lies the disadvantage of the parallel arrangement of the cell members. The total separation achieved by the cell will always be an average of the separations achieved by each of the individual cells. Therefore, if one bad cell member is present in the assembly, the entire assembly will also be unsatisfactory. For this reason an attempt was made to test the continuity of the films of the individual cell members before they were used for construction purposes. This test consisted of a visual inspection of each film surface and permeability measurements similar to those used for the unlaminated films.

The Cell 3A, which was used in the test, had an overall volume of 345 cm^3 (2.54 x 11.42 x 11.42) which includes the potting material. This volume contained a combined film surface of 640 cm^2 having an average thickness of 0.0206 cm (8 mil). Figure 16 of the appendix depicts the flow capacity of both the laminated and unlaminated substrates for this cell. Figure 17

shows the capacity of the unlaminated substrates for several cells. The maximum pressure drop exerted across the membranes was approximately 760 mmHg. On the high pressure side the feed was admitted and the wastes expelled at slightly above atmospheric pressure. The low pressure side was kept at 10 mmHg. vacuum throughout the test run.

In order to test the flexibility of the model cells with respect to pressure, several of them were subjected to tests in which the upstream pressure was greater than atmospheric. These tests demonstrated that this particular cell design is somewhat inflexible with regard to pressure. For upstream pressures greater than 5 psia, bond breakage and leaks quickly developed within the assembly. To overcome this lack of flexibility a slightly different cell design was created. However, this new design was never completely developed and tested. A schematic representation appears in Figures 25 and 26 of the Appendix, together with a brief discussion of it.

CONCLUSIONS

The basic purpose of this investigation was to study the feasibility of the proposed permeability cell. It is hoped that the data herewith presented not only attest to the feasibility of the cell, but also to its functionability. This is not meant to imply, however, that all the problems have now been solved. On the contrary, they have not.

With respect to membranes which are available at the present time, the 5 to 1 separation ratio achieved by the silicone rubber elastomer for carbon dioxide and oxygen was considered quite satisfactory. From the theoretical view point, however, this is not so. Separation factors of 10,100, or 1000 times this value are much more desirable. For this reason, a continual search for new polymers is necessary; if the best possible membrane is to be obtained.

The film thickness in the test cell 3A was purposely kept at an 8 mil thickness in order to make certain that no leaks would develop during the test runs. However, this is much too thick for actual cell operation. Films as thin as 0.25 mil would be much more desirable. Therefore better methods of preparing thin films are also needed. Films as thin as 1.5 to 2 mils were prepared by the drawing knife procedure during the experiment.

However, the presence of dust in the air, which settled on the films produced inconsistencies in these films making them unusable for cell construction. With the lamination technique described in the theoretical section, General Electric has, on the other hand, had relatively good success in making consistent films 0.5 mil in thickness with silicone rubbers.

Although the substrate which was used in the cell was quite porous and performed well, it was also quite bulky with a thickness of 6 mil. As with the film thickness, the substrate should be kept as thin as possible, without sacrificing porosity, if a volume saving is to be realized. Thus a continuing search for better substrates is also needed.

The basic design proposed for the cell, and the method of connecting the individual cell members in parallel proved to be both practical and workable. The units were not too difficult to assemble and worked as predicted. In most instances the ratio of the film area to cell volume was not exceptionally high for most of the cells tested. However, it was felt that this type of cell design improved on existing methods, and would be even more effective with continued research on construction methods and materials.

It will be recalled that the pure gas permeabilities indicated that a better separation ratio could be

obtained at lower temperatures. It was not ascertained, however, that the optimum operating conditions of the cell were also at these low levels. If the permeability coefficient of carbon dioxide is truly constant with temperature, then the optimum conditions should be at the lower temperature levels. For this reason more experimentation below the 0°C level would be desirable.

APPENDIX

TABLE 4

Typical Data For Permeability Measurement

Cell #6 K (cell constant) = 359,000 x 10^{-9} (Major's Compact Apparatus)

Sample RTV-501 Pure Gas CO_2

Barometric Pressure 1. 750 mm Hg

Temperature 27°C

F Correction factor = 1.003

h = 20.0 in. Hg (9.84 psi)

Film Thickness (L) 3.75 (avg. mil) or 0.0146 cm

	Scale Divisions Slug Travels (S)	Time Sec (θ)	(S/θ) avg
1.	14	24	
2.	14	24	0.56
3.	14	25	
4.	14	24	
5.	14	25	
6.	14	25	
7.	14	25	

$P = \frac{KFL}{h} (S/\theta) = 299 \times 10^{-9}$ c.g.s. units

TABLE 5

Typical Data for Substrate Porosity Measurement

Sample Paper Towel

Barometric Pressure 749 mm Hg

Temperature 27°C

Sample Thickness 6.2 mils or 0.0157 cm

Run	Units Slug Travels	Time θ Sec	Δ P mm Hg	$(2/\theta\Delta P) \times 10^3$ (cc/sec)(1/mmHg)
1	2	61.3	0.964	33.9
2	2	62.9	0.960	33.2
3	2	50.7	1.05	37.6
4	2	53.3	1.04	36.1
5	2	61.5	0.99	32.9
6	2	54.2	1.00	36.7
7	2	57.7	1.00	34.7
8	2	65.0	0.953	31.9
9	2	55.5	1.03	35.2
10	2	54.8	1.03	35.6
				34.78 avg

Apparant Porosity (avg) = (34.78/15.7) = 2.21 cc/(sec)(cm)(mmHg)

TABLE 6

Unique Perm Cell Separation Tests

Cell 3A

Feed Cone 90.2 O_2

Bath 40°C

Barometric Pressure 750 mm Hg

Run	F(cc/min)	W(cc/min)	(1-W/F)	XpO_2	$XpCO_2$	Press. Product Side
1	24.0	12.0	0.50	0.816	0.184	95.7mm Hg
2	17.0	8.0	0.53	0.825	0.175	
3	10.5	4.0	0.619	0.835	0.165	
4	7.5	3.0	0.625	0.845	0.155	
5	6.0	1.8	0.700	0.870	0.130	
6	18.0	8.7	0.517	0.818	0.182	
7	9.0	3.4	0.622	0.846	0.154	

Max. CO_2 in Product 35.6%*

* Max. product compositions were predicted with equation 3, p. 24.

TABLE 7

Unique Perm Cell Separation Tests

Cell 3A

Feed Cone 93% O_2

Bath 40°C

Barometric Pressure 748 mm Hg

Run	F(cc/min)	W(cc/min)	Φ (1-W/F)	XpO_2	$XpCO_2$	Press. Product Side
1	35.0	21.5	0.385	0.83	17.0	98.7
2	19.5	10.0	0.487	0.85	15.0	
3	9.2	3.6	0.608	0.882	11.8	
4	6.0	1.7	0.716	0.904	9.6	
5	11.0	4.8	0.564	0.885	11.5	
6	25.0	13.0	0.480	0.857	14.3	

Max. CO_2 in Product 27.3%

TABLE 8

Unique Perm Cell Separation Tests

Cell 3A

Feed Cone 99% O_2

Bath 40°C

Barometric Pressure 742 mm Hg

Run	F(cc/min)	W(cc/min)	Φ (1-W/F)	XpO_2	$XpCO_2$	Press. Product Side
1	142	135	0.05	0.958	0.042	93.7 mmHg
2	121	111	0.082	0.972	0.028	
3	94	83	0.116	0.978	0.022	
4	72	61	0.153	0.981	0.019	
5	45	33.9	0.270	0.989	0.011	
6	24	13.5	0.438	0.990	0.010	

Max. CO_2 in Product 4.8%

TABLE 9

Unique Perm Cell Separation Tests

Cell 3A

Feed Cone 92% O_2

Bath 25°C

Barometric Pressure 740 mm Hg

Run	F(cc/min)	W(cc/min)	Φ (1-W/F)	XpO_2	$XpCO_2$	Press. Product Side
1	20	11.7	0.415	0.810	0.190	
2	15	7.9	0.474	0.828	0.172	
3	10	4.8	0.520	0.845	0.155	94.6mm Hg
4	8.5	3.6	0.576	0.854	0.146	
5	7.0	2.8	0.600	0.876	0.124	
6	5.8	2.0	0.625	0.885	0.115	

Max. CO_2 in Product 30.3%

TABLE 10

Unique Perm Cell Separation Tests

Cell 3A

Feed Cone 94% O_2

Bath 25°C

Barometric Pressure 740 mm Hg

Run	F(cc/min)	W(cc/min)	Φ (1-W/F)	XpO_2	$XpCO_2$	Press. Product Side
1	50.5	41	0.19	0.835	0.165	
2	36.0	26	0.28	0.840	0.160	94.9mm Hg
3	23.5	12.8	0.455	0.860	0.140	
4	7.6	3.6	0.525	0.865	0.135	
5	5.5	1.9	0.64	0.900	0.100	
6	10.0	5.1	0.49	0.875	0.125	

Max. CO_2 Product 24.2%

TABLE 11

Unique Perm Cell Separation Tests

Cell 3A

Feed Cone 98% O_2

Bath 25°C

Barometric Pressure 740.1 mm Hg

Run	F(cc/min)	W(cc/min)	Φ (1-W/F)	XpO_2	$XpCO_2$	Press. Product Side
1	97	87	0.102	0.935	0.065	
2	81	71	0.124	0.944	0.056	95.9 mm Hg
3	59	50	0.154	0.946	0.054	
4	33	24	0.272	0.954	0.046	
5	15	9.0	0.400	0.961	0.039	
6	11	6.4	0.428	0.969	0.031	
7	9.5	5.3	0.497	0.976	0.024	

Max. CO_2 in Product 9.3%

TABLE 12

Unique Perm Cell Separation Tests

Cell 3A

Feed Cone 91% O_2

Bath 0°C

Barometric Pressure 745 mm Hg

Run	F(cc/min)	W(cc/min)	Φ (1-W/F)	XpO_2	$XpCO_2$	Press. Product Side
1	32.5	24.0	0.26	0.81	0.190	95.9 mmHg
2	26.0	18.5	0.288	0.81	0.190	
3	20.0	12.0	0.400	0.829	0.171	
4	15.0	8.5	0.433	0.835	0.165	
5	13.2	7.3	0.447	0.845	0.155	
6	7.5	4.1	0.454	0.843	0.157	
7	5.0	2.0	0.600	0.890	0.110	

Max. CO_2 in Product 33.1%

TABLE 13

Unique Perm Cell Separation Tests

Cell 3A

Feed Cone 95.5% O_2

Bath 0°C

Barometric Pressure 747 mm Hg

Run	F(cc/min)	W(cc/min)	Φ (1-W/F)	XpO_2	$XpCO_2$	Press. Product Side
1	47	44	0.065	0.892	0.108	95.5mm Hg
2	24	21	0.125	0.895	0.105	
3	18	14	0.222	0.908	0.92	
4	12	7.5	0.375	0.911	0.89	
5	8	4.5	0.437	0.920	0.80	
6	6.1	3.2	0.475	0.924	0.76	

Max. CO_2 in Product 19.07%

TABLE 14

Unique Perm Cell Separation Tests

Cell 3A

Feed Cone 98% O_2

Bath 0°C

Barometric Pressure 748 mm Hg

Run	F(cc/min)	W(cc/min)	Φ (1-W/F)	XpO_2	$XpCO_2$	Press. Product Side
1	145	143	0.014	0.939	0.061	
2	121	118	0.025	0.940	0.060	95.7 mm Hg
3	94	92.0	0.020	0.949	0.051	
4	72	70.0	0.028	0.944	0.056	
5	24	21.0	0.125	0.960	0.040	
6	6.5	3.0	0.538	0.976	0.024	
7	15.0	12.8	0.145	0.970	0.030	
8	7.0	4.8	0.315	0.972	0.028	

Max. CO_2 in Product 9.25%

TABLE 15

Typical Data for Permeability Cell Separation

Run #1 Cell 3-A Feed Concentration 98% O_2

Bar. Press. 740.1 mm Hg Bath 25°C Date April 17, 1964

Run	Feed Rotameter	Waste Rotameter	Manometer	O_2 Peak Height
1	9.0	41.5	92.8 mm Hg	440.0
2	8.3	36.5	95.0	455.0
3	7.4	30.0	95.0	456.0
4	6.3	19.0	92.8	449.5
5	5.3	10.5	90.7	443.0
6	4.9	8.0	95.0	466.5
7	4.75	7.0	89.0	440.5

Feed 1* 472.5 O_2 peak, 93.2 mm Hg Manometer reading

7* 475.5 O_2 peak, 93.7 mm Hg Manometer reading

FIGURE II
SEPARATION CURVES
(40° C) (O_2- CO_2) (CELL 3-A)

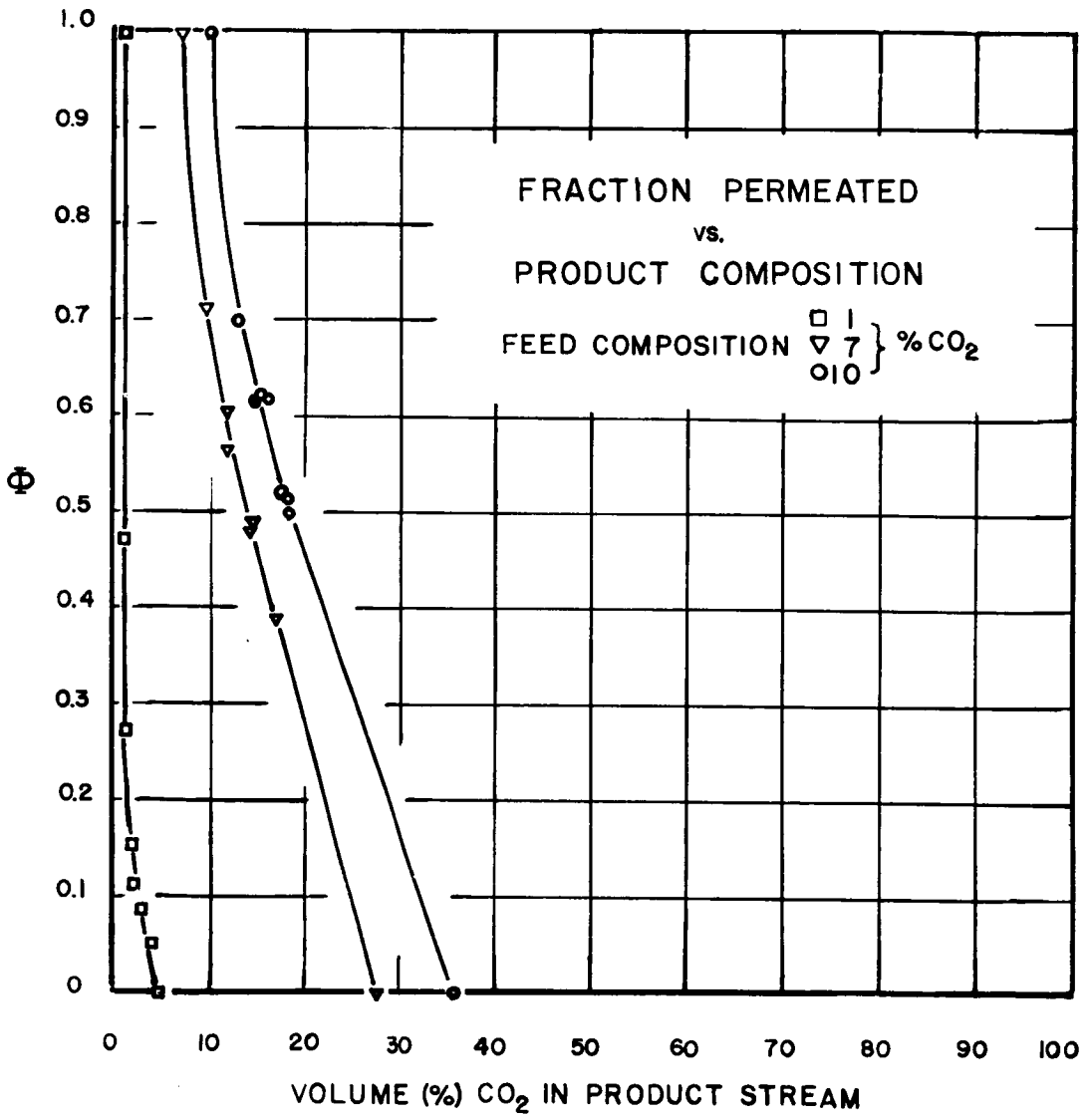

FIGURE 12

SEPARATION CURVES

(25° C) (O_2-CO_2) (CELL 3-A)

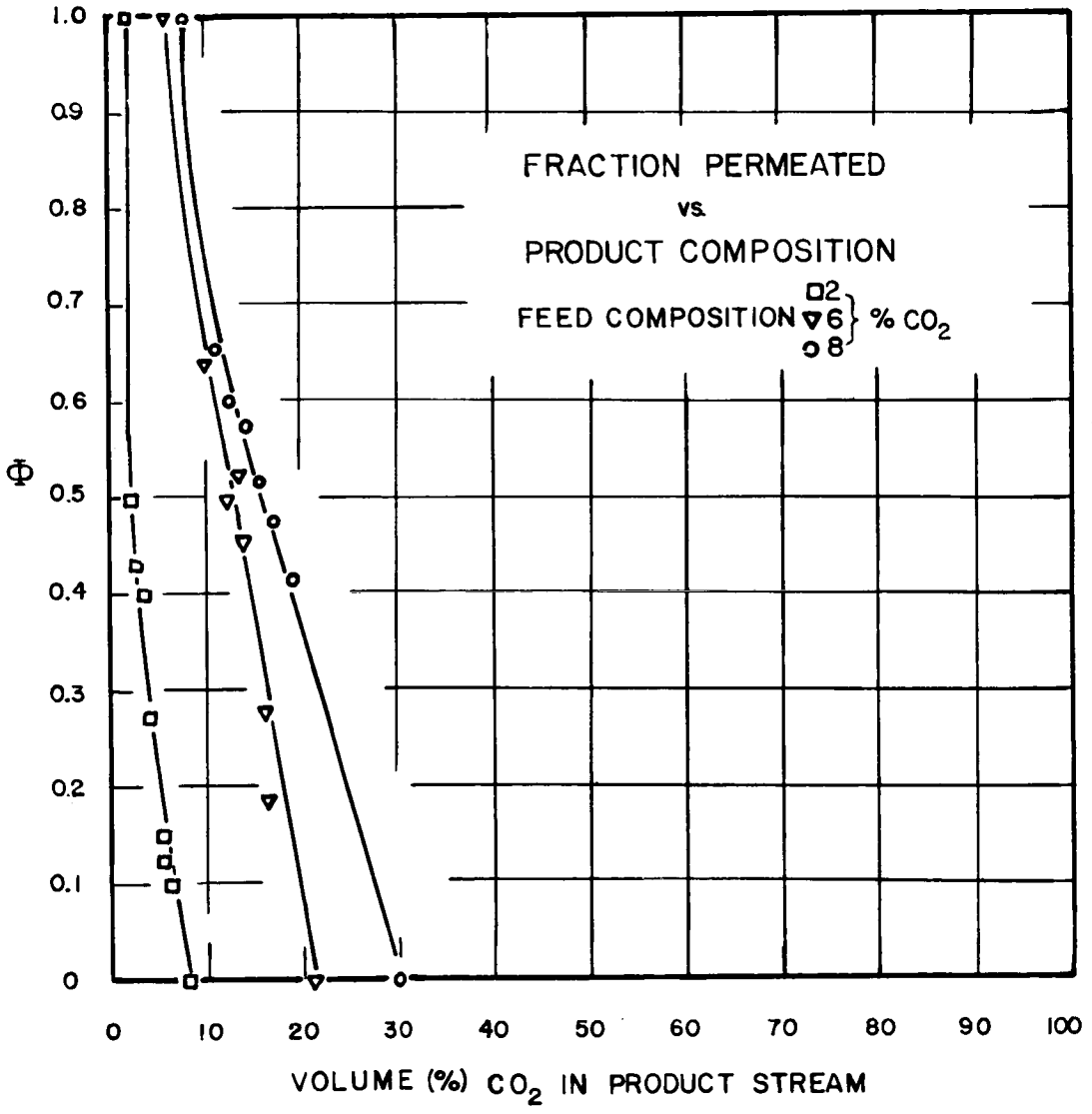

FIGURE 13
SEPARATION CURVES
(0° C) (O_2-CO_2) (CELL 3-A)

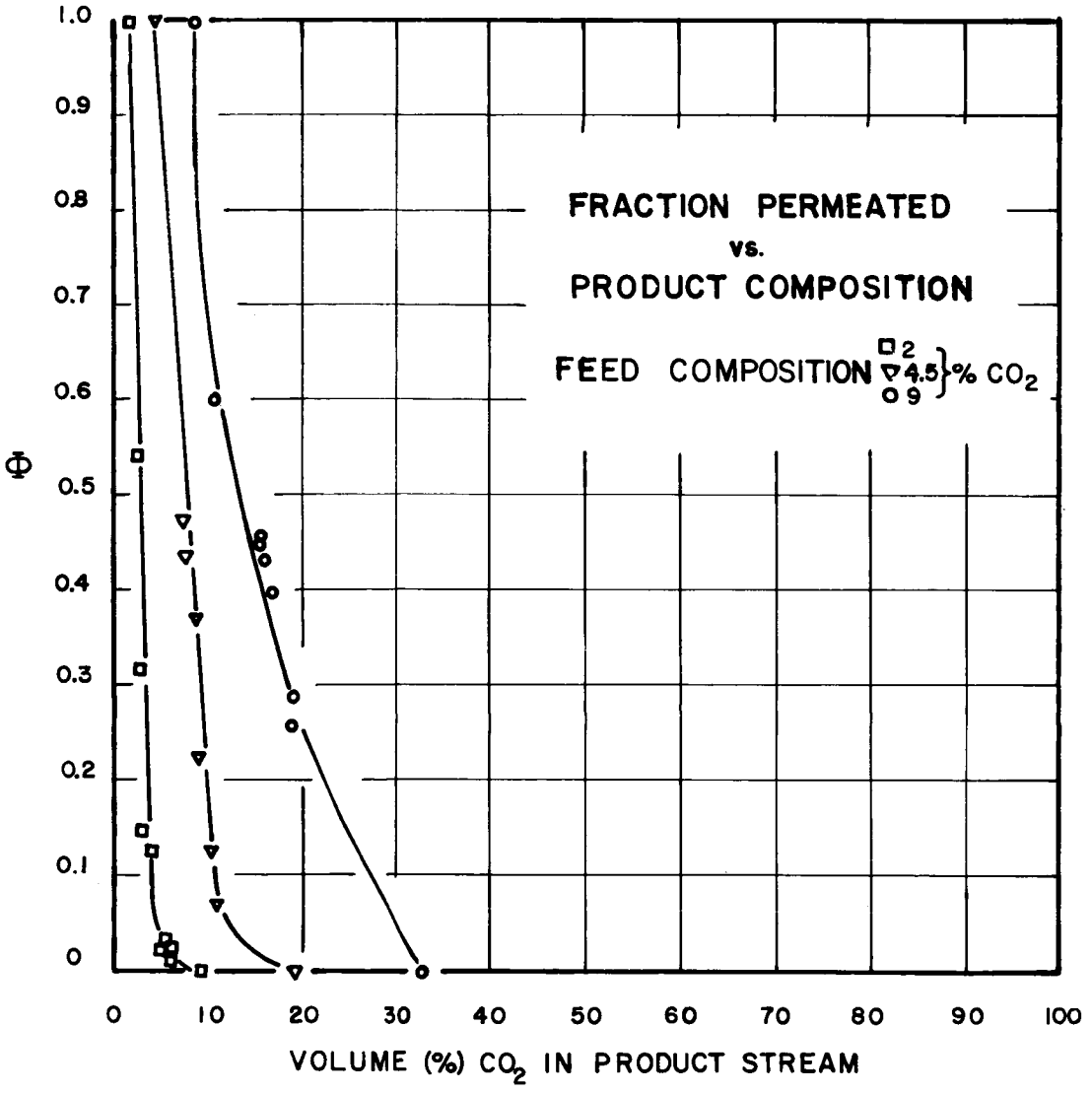

FIGURE 14

ACTUAL AND THEORETICAL SEPARATIONS

(40°C) (O_2-CO_2) (CELL 3-A)

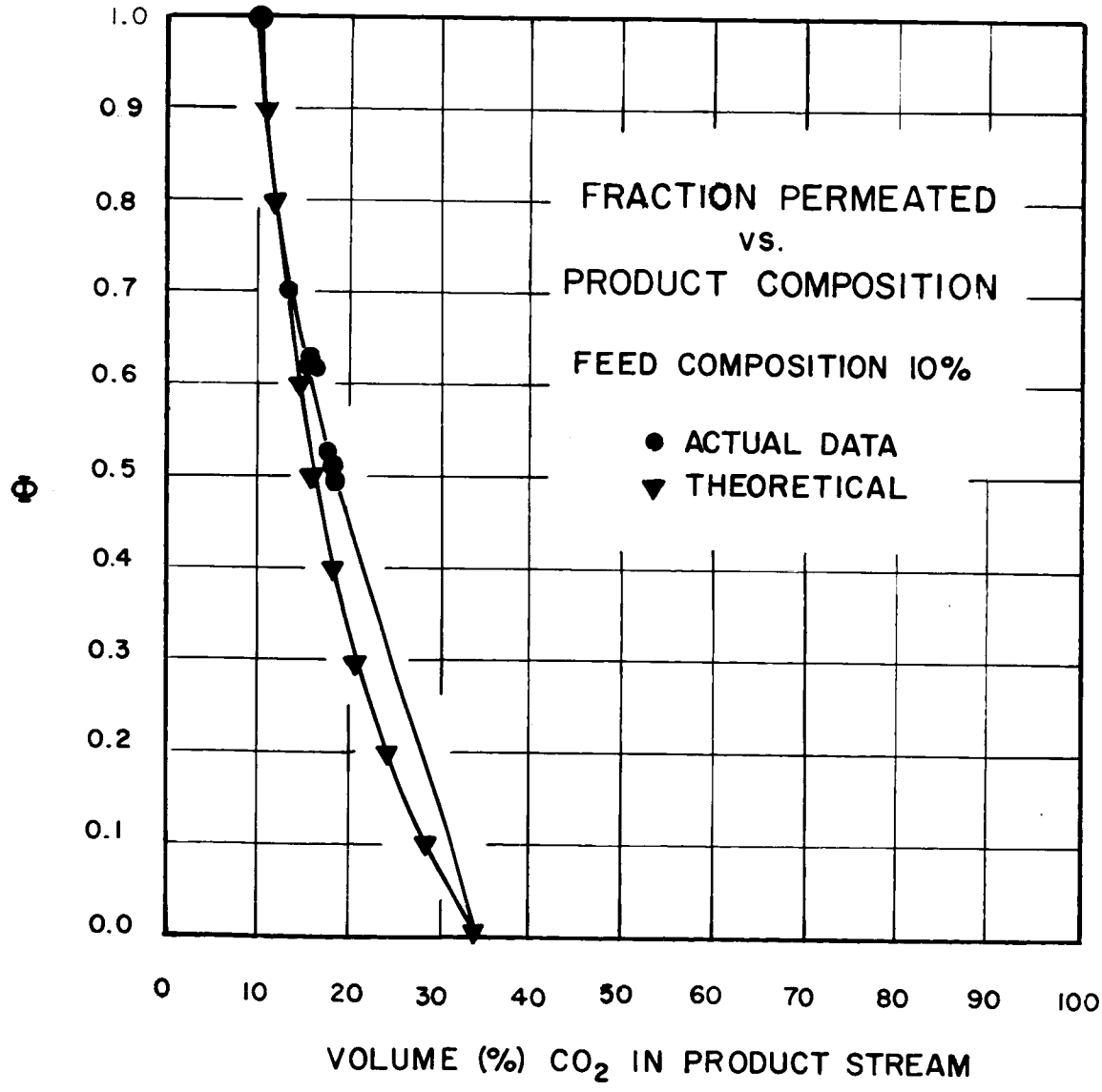

TABLE 16

Capacity of Permeability Cell Substrates

Feed and Waste Substrate			Product Substrate		
ΔP(mm Hg)	Q(ft^3/min)	($\frac{ft^3}{min}$ $\frac{in}{in^2}$)	ΔP(mm Hg)	Q(ft^3/min)	($\frac{ft^3}{min}$ $\frac{in}{in^2}$)
25.4	0.19	6.93	25.4	0.0096	0.35
38.1	0.282	10.28	50.8	0.0191	0.70
50.8	0.356	12.98	76.2	0.0311	1.13
63.5	0.435	15.85	101.5	0.0454	1.66
76.2	0.503	18.34	127.0	0.0634	2.31
89.0	0.571	20.82	152.3	0.0735	2.68
101.5	0.604	22.02	152.3	0.0735	2.68
114.2	0.638	23.26	178.0	0.0910	3.32

FIGURE 15

APPARATUS FOR MEASURING SUBSTRATE CAPACITY

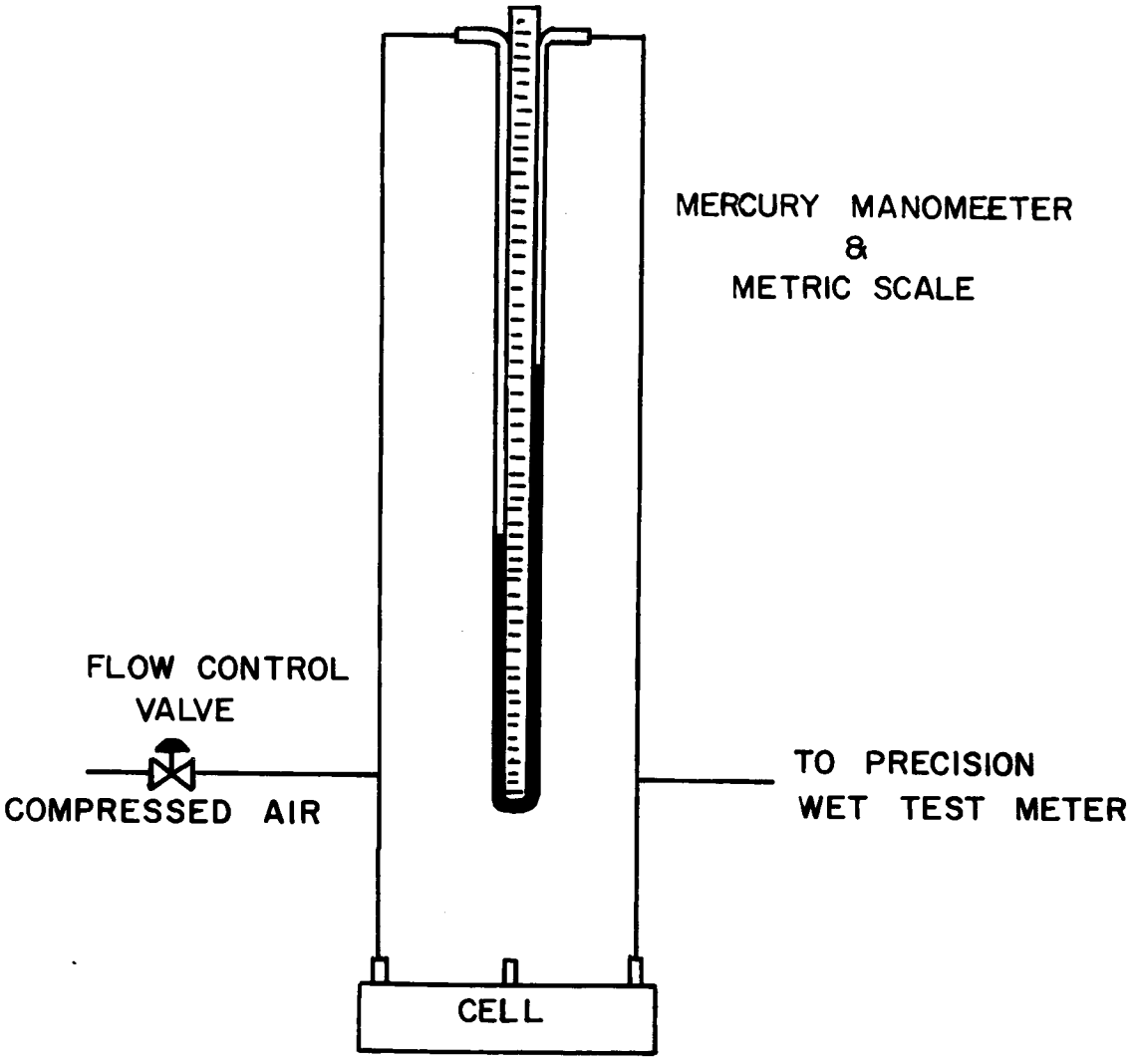

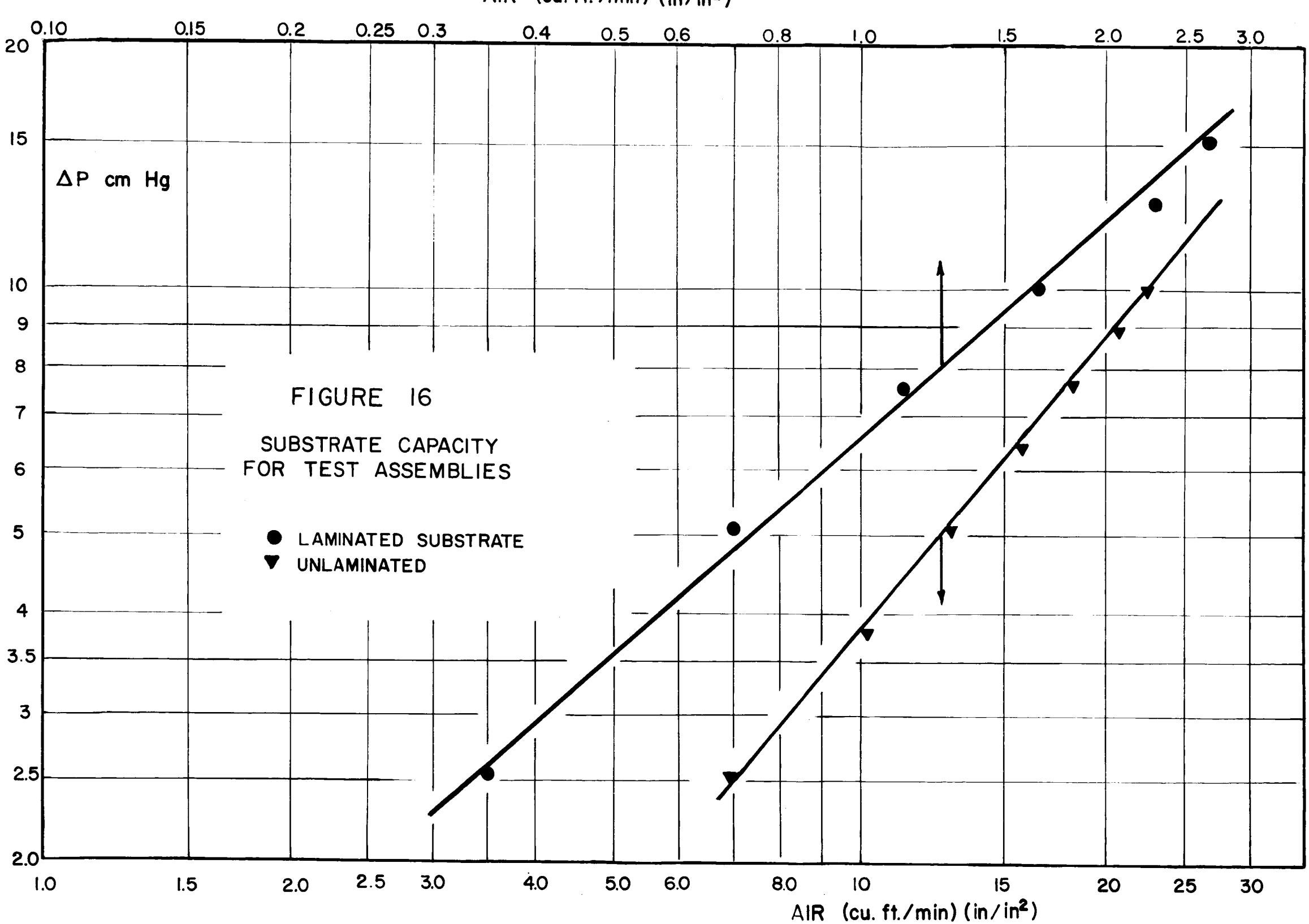
AIR (cu. ft./min) (in/in²)
0.10
0.15
0.2
0.25
0.3
0.4
0.5
0.6
0.8
1.0
1.5
2.0
2.5
3.0
20
15
10
9
8
7
6
5
4
3.5
3
2.5
2.0
ΔP cm Hg
FIGURE 16
SUBSTRATE CAPACITY
FOR TEST ASSEMBLIES
LAMINATED SUBSTRATE
UNLAMINATED
1.0
1.5
2.0
2.5
3.0
4.0
5.0
6.0
8.0
10
15
20
25
30
AIR (cu. ft./min) (in/in²)

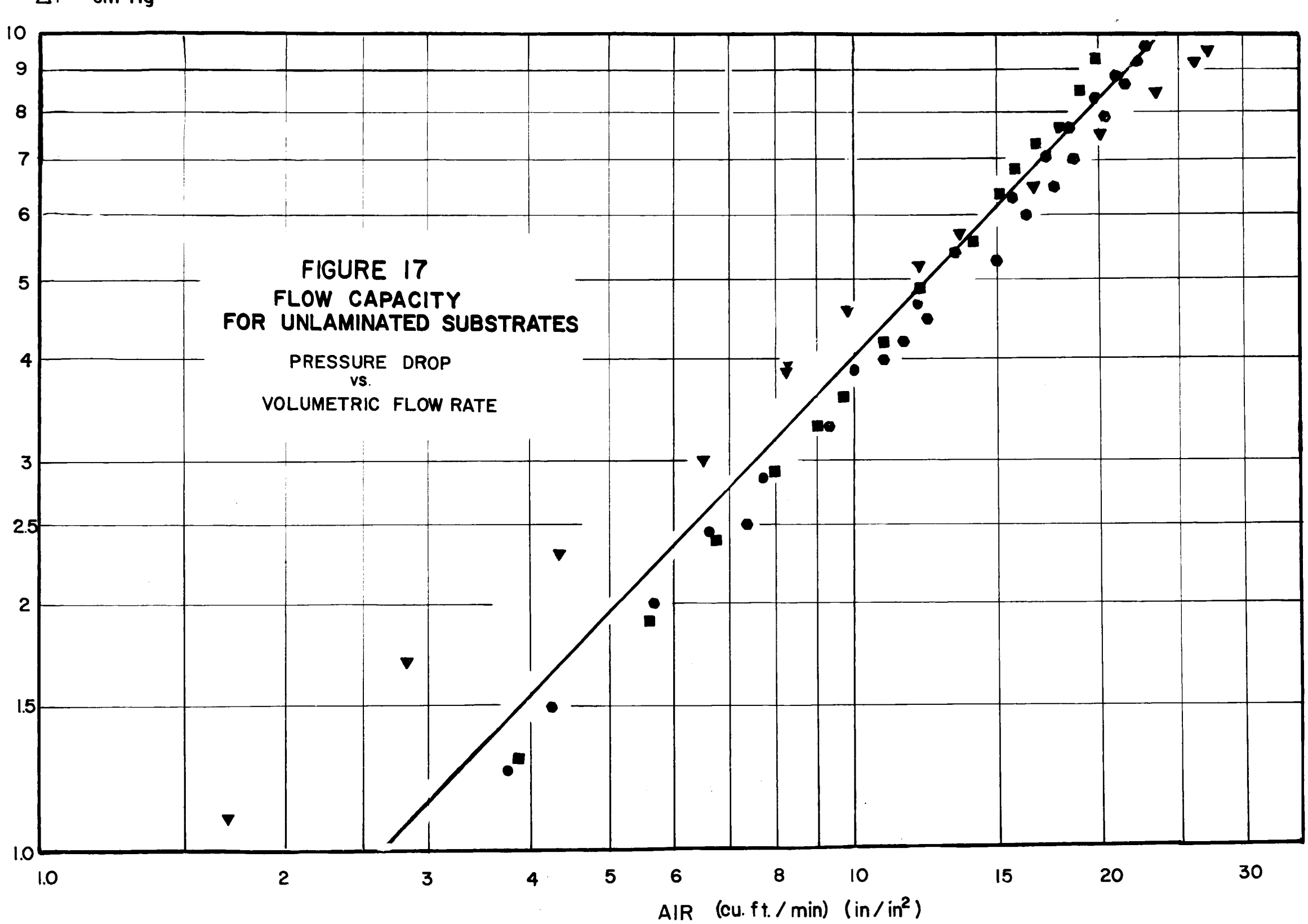

FIGURE 17
FLOW CAPACITY
FOR UNLAMINATED SUBSTRATES

PRESSURE DROP
vs.
VOLUMETRIC FLOW RATE

FIGURE 18 Barometric Permeability Apparatus C. J. Major

FIGURE 19 Volumetric Compact Permeability Apparatus C. J. Major

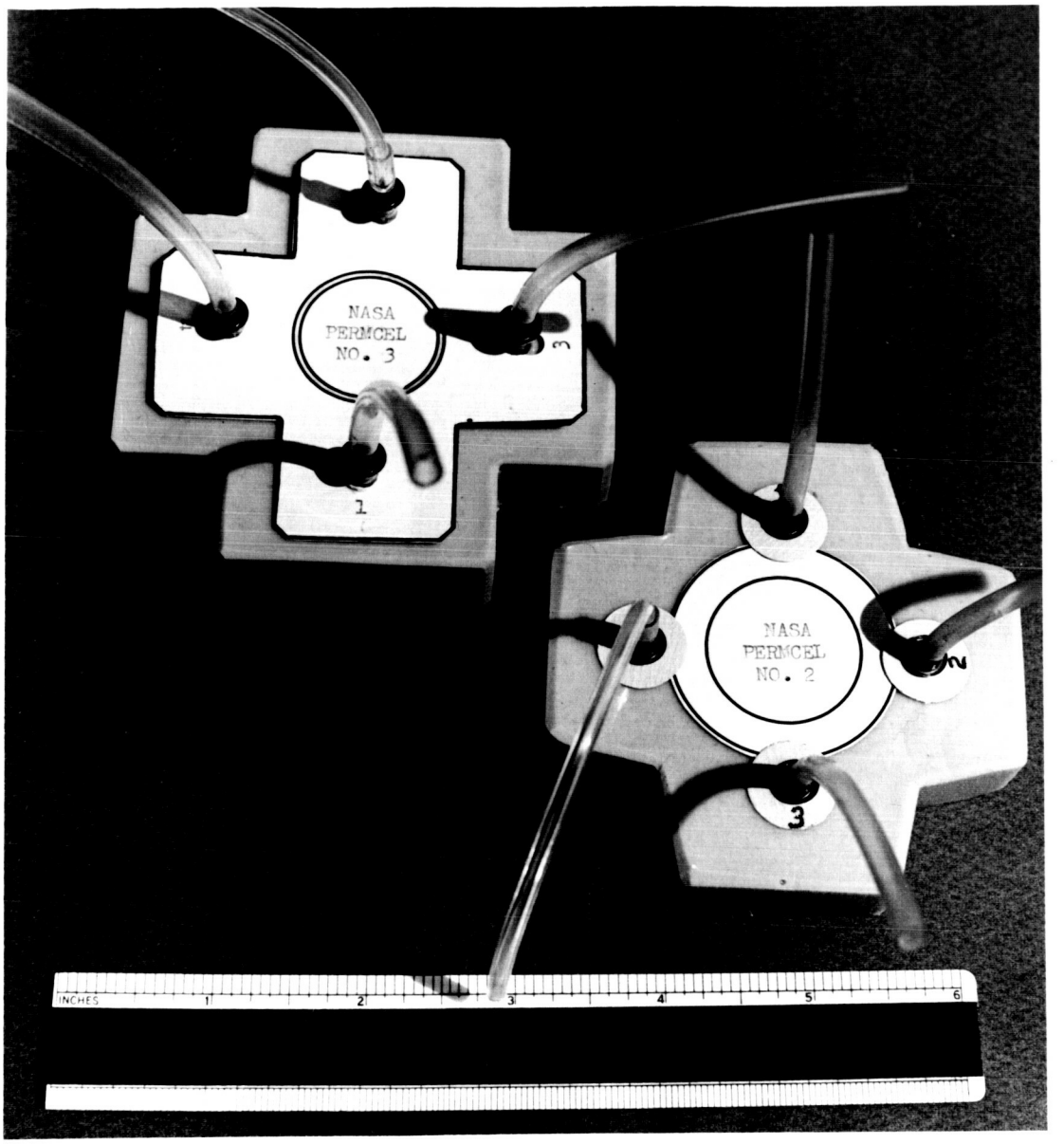

FIGURE 20 Early Permeability Assemblies.
Cells Are Potted in Silastic Silicone Rubber.

FIGURE 22 Permeability Cell in temperature bath during actual test run.

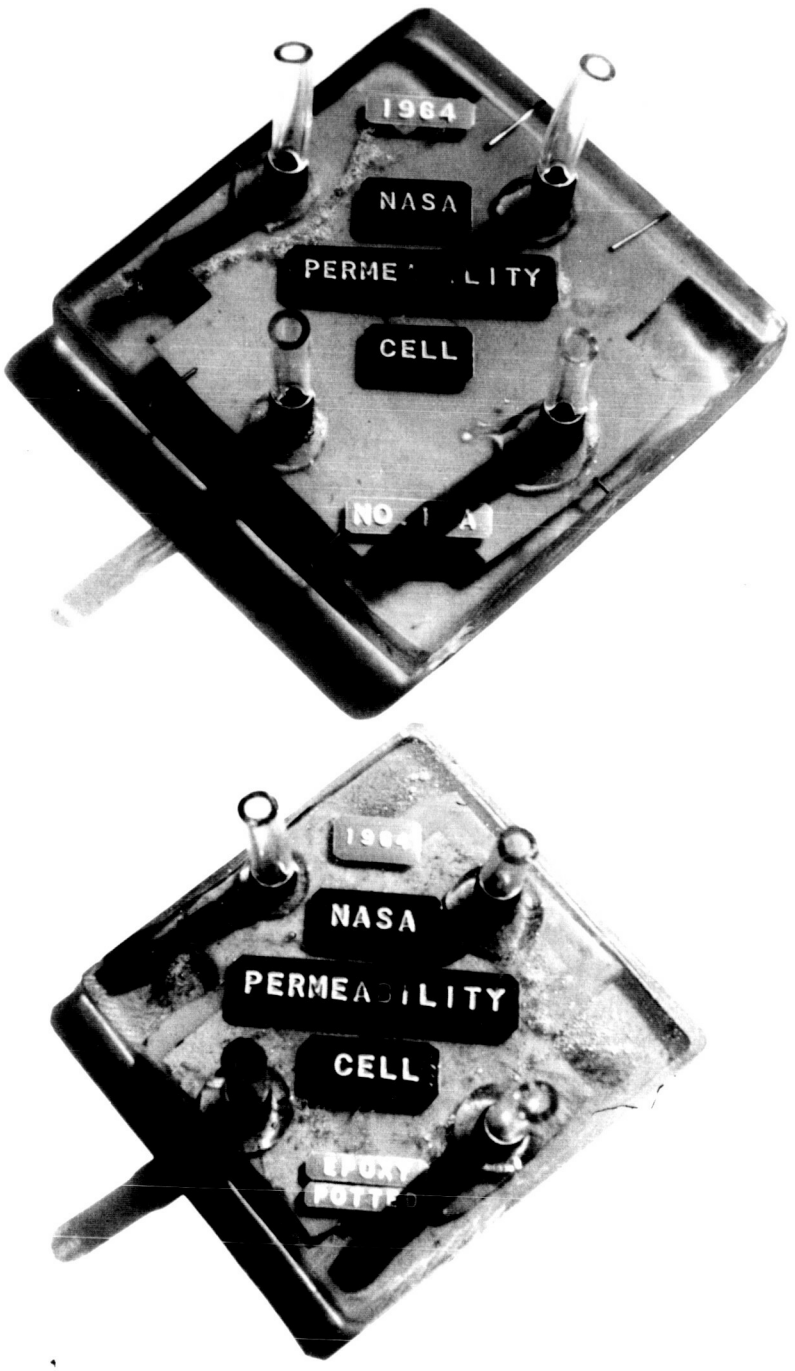

FIGURE 21 Permeability Cells

Potted in epoxy resin.

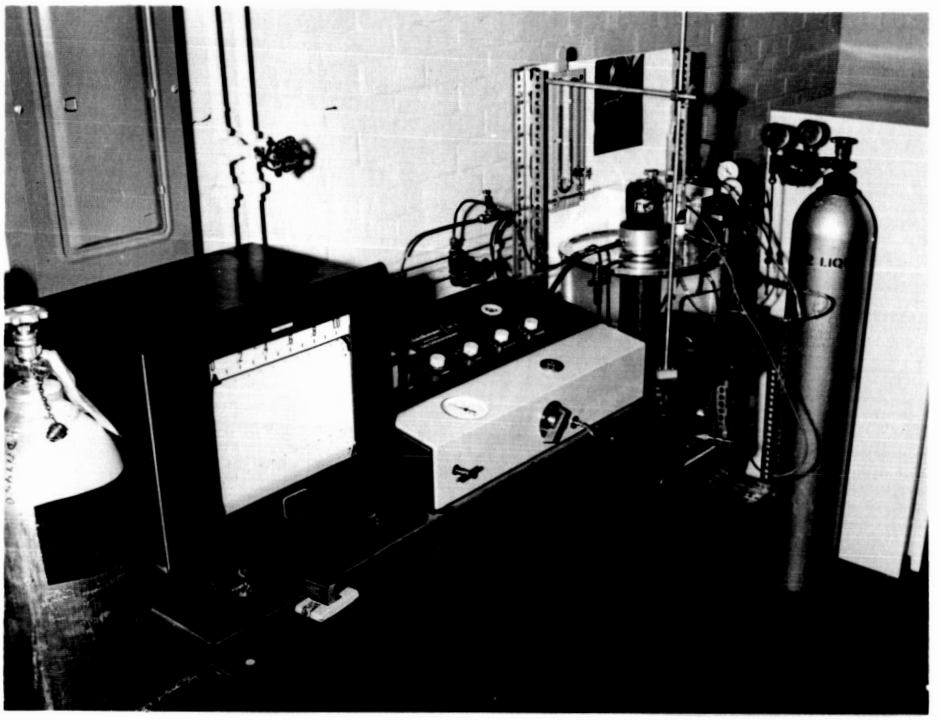

FIGURE 23 Cell Testing Apparatus

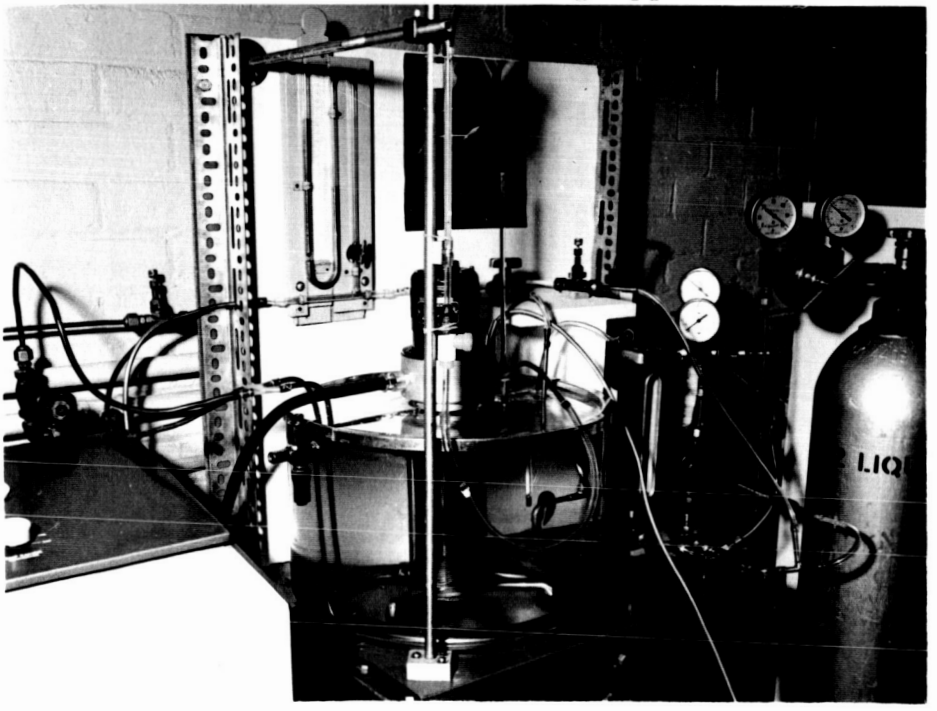

FIGURE 24 Cell Testing Apparatus

LEGEND FOR FIGURES 8, 23, 24

1. Gas Chromatograph
2. Valve
3. Cold Trap
4. Manometer
5. Valve
6. Valve
7. Thermometer
8. Temperature Conditioning Coils
9. Waste Rotameter (Roger Gilmont A 927)
10. Constant Temperature Bath
11. Permeability Cell
12. Feed Rotameter (Fisher Porter, SUI #47682)
13. Bleed Valve
14. Oxygen Flow Control Valve
15. Gas Proportioner

CALCULATIONS

1. A porosity value for a substrate sample is computed from the following equation.

$$\Psi = (V)/(\theta)(Z)(\Delta P)$$

Where Ψ is the apparent porosity of the sample

V is the scale divisions which the slug travels (this is proportional to the volume permeated)

θ is the time in seconds for V scale divisions of slug travel

Z is the thickness of the substrate (cm)

ΔP is the pressure drop required to produce the rate V/θ (mm Hg)

The relative porosity of a substrate sample is computed by the following equation.

$$\Psi_r = \Psi / \Psi_s$$

Ψ_r relative porosity

Ψ apparent porosity

Ψ_s porosity standard

Example 1. Calc. Porosity of Paper Towel

$$\Psi = (V)/(\theta)(Z)(\Delta P)$$

From Table 5, page 44

$V = 2$; $\theta = 61.3$; $Z = 0.0157$; $\Delta P = 0.964$

$= (2)/(61.3)(0.0157)(0.964)$

$= 2.16$ (divisions)/(sec)(cm)(mm Hg)

Example 2. Calc. Relative Porosity of Paper Towel

$$\Psi_r = \Psi / \Psi_s$$

Lined writing paper is used as a standard and has a porosity of 0.252.

$$\Psi = 2.16$$

$$\Psi_s = 0.252$$

$$\Psi_r = 2.16/0.252 = \underline{8.58}$$

2. Weller Steiner Case I derivation for a unit area of membrane Fick's Law: $dxp = \bar{P}_1 (PXo - PXp)$ Change of Component 1

$$d(1 - xp) = \bar{P}_2 (P(1-Xo) - P(1 - Xp))$$ Change of Component 2

Dividing these equations

$$\frac{Xp}{1-Xp} = \alpha \frac{(PXo - PXc)}{P(1 - Xo) - P(1 - Xp)}$$

From material and component balances the general equation becomes a quadratic whose solution is

$$Xp = \frac{-b + \sqrt{b^2 - 4ac}}{2a}$$

For the specific case of maximum product composition or zero product take off

$$Xo \longrightarrow X_F$$

$$P \longrightarrow 0 \qquad \frac{Xp}{1 - Xp} = \alpha \frac{(PXo)}{P(1 - Xo)} = \frac{X_F \alpha}{(1 - X_F)} \qquad (3)$$

Example 3. Calc. Maximum product composition for feed containing 10% carbon dioxide. Assume a separation factor of $\alpha = 5.0$. (Calculated α equals $(\bar{P}_1/\bar{P}_2)$ at test temperature) $XF = 0.10$

From Eq. (3), p. 89; $\left(\frac{Xp}{1 - Xp}\right) = \frac{(5)(0.10)}{(9.90)} = \frac{0.50}{0.90}$

$$0.90\ Xp = 0.50 - 0.50\ Xp$$

$$1.40\ Xp = 0.50$$

$$Xp = 35.7\%\ CO_2$$

3. Calculation of Product Composition

The product composition is calculated from the peak height data recorded on the gas chromatograph.

$$Xp = \frac{\text{Partial Pressure}}{\text{Sample Pressure}}$$

The partial pressure is indicated by the peak height recorded by the gas chromatograph. The peak height of the pure gas must first be calibrated at various pressures over the range of sample pressures being used. A plot of peak height versus sample pressure is drawn for each pure gas. Then the pressure corresponding to the component peak height of the sample is the partial pressure of that component in the sample.

4. Calculation of the Cut Φ

$$\Phi = \frac{\text{Product rate}}{\text{Feed rate}} = 1 - \frac{\text{Waste rate}}{\text{Feed rate}}$$

The waste rate and feed rates are obtained from rotameter readings and calibration curves of rotameter reading vs. flow rate.

Example 4. Calculation of the product composition for cell separation. From Table 15; Run #1*, Manometer = 92.8 mm Hg.

O_2 Peak Height = 440

From the calibration curve an oxygen peak height of 440 represents a pressure of 86.6 mm Hg

$$X_{P_{O_2}} = \frac{P_{O_2}}{\overline{P}} = \frac{86.6}{92.8} = 93.4\% \; O_2$$

Example 5. Calculation of the Cut Φ . From Table 15:

Run #1*, Feed Rotameter 9.0 = 97 cc/min

Waste Rotameter 41.5 = 87 cc/min

$\Phi = 1 - 87/97 = 0.102$

5. Calculation of Cell Substrate Capacity

$$\text{Capacity } C = \frac{Q1}{AN}$$

where Q = volumetric flow rate (ft^3/min)

L = length of a single substrate (in)

A = cross-sectional area for a single substrate (in^2)

N = number of substrate layers

NOMENCLATURE

α ratio of pure gas permeabilities $(\overline{P}_A/\overline{P}_B = \alpha_{AB})$

a constant for solution of Weller Steiner Case I equation

$$(\alpha - 1)(P + \Phi \Delta P)$$

b constant for solution of Weller-Steiner Case I equation

$$\left[(\alpha - 1)(-\Phi X_F - \Delta P) - \Phi \Delta P - \alpha P\right]$$

C constant for solution of Weller-Steiner Case I equation

$$\Phi \alpha X_F$$

ΔP absolute pressure drop across the cell membranes $(\Phi - P)$ = psia

Φ pressure on high pressure side of the membrane (psia)

P pressure on low pressure side of the membrane (psia)

$\overline{P}$ permeability constant (std cc - cm/cm^2 - sec - cm Hg)

Φ ratio of product flow rate to feed flow rate or the cut

X_F mole fraction of carbon dioxide in feed stream

X_o mole fraction of carbon dioxide in waste stream

Xp mole fraction of carbon dioxide in product stream

High Pressure, Permeability Cell Design

Figures 25 and 26 show the basic construction of the proposed high pressure cell design. As shown in Figure 25, the cell is housed in a metalic cylinder which is capped at both ends. The cylinder is tapped with the appropriate ports to permit the flow of feed, waste, and product streams, and to facilitate mixing of the feed gases, if desired. This capped metalic cylinder permits the use of higher pressures than were possible with the old assemblies which were coated only with expoxy resin.

Figure 26 shows that the actual separation assembly has a cylindrical shape. This exploded view also depicts the structure of the multi-layered unit. Each of the basic separation units is a circular piece of filter paper sealed within a circular envelope of silicone film. A piece of this same filter paper is placed between each of these basic separation units. This permits a freer flow of the feed gases in the vicinity of the film surfaces thereby facilitating permeation. As with the old assemblies, the product stream is withdrawn from a duct tapped through the assembly. The product stream is kept separate from the feed and waste streams by the use of a heat exchanger coupling. Swagelok fittings are required at all joints to reduce the possibilities of leaks.

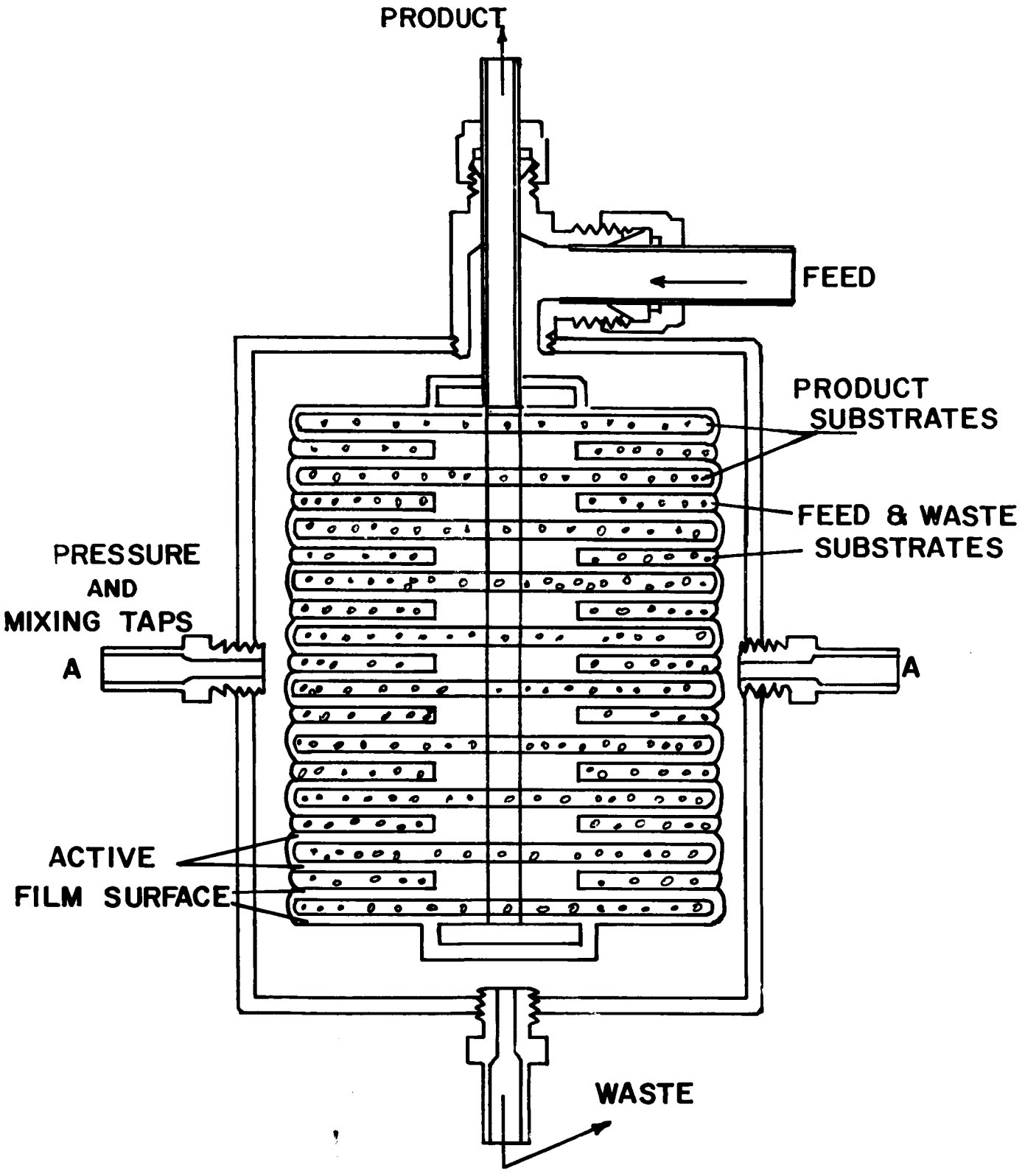

FIGURE 25

SEPARATION CELL

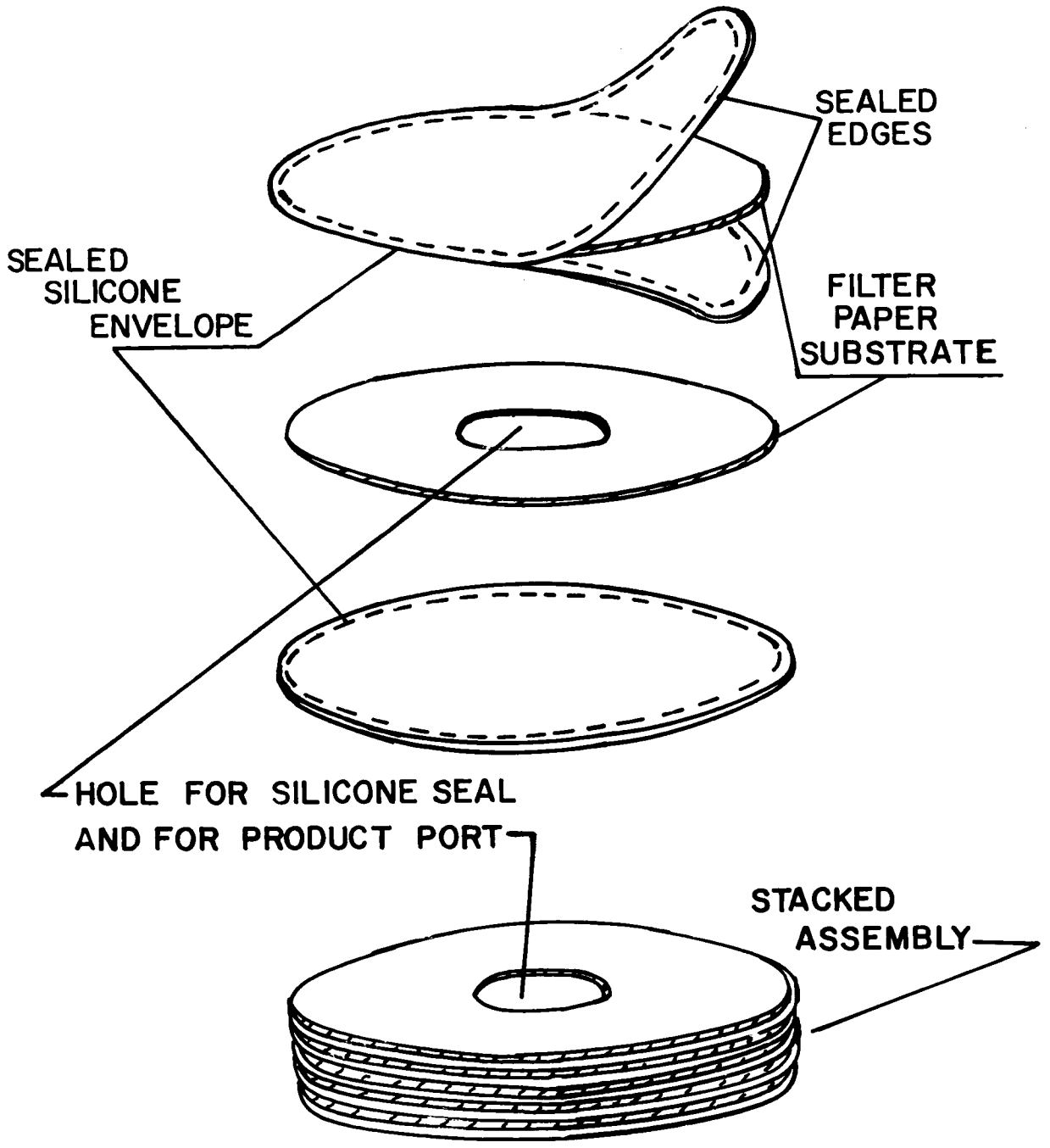

FIGURE 26

VIEW OF LAYERED ASSEMBLY

Computer Solution for Weller Steiner Case I

As shown in the theoretical section, pages 22 and 23, the Weller Steiner Case I model for a binary system can be reduced to a simple quadratic equation:

$$X_p = \frac{-b + \sqrt{b^2 - 4ac}}{2a}$$

Where the valves of a, b, and c are given on pages 23 and 93. Solutions to this equation were obtained using the digital computer. The Fortran notation which was used, and the nomenclature associated with it are listed below. The object of the program was to observe the effect a change in cut (ϕ) has upon the product composition. For this reason all the remaining variables were fixed. Table 17 shows some of the results of the program. This table is tabulated as product composition versus cut for a number of feed concentrations.

```
C     TOCK, R.W.  WELLER STEINER CASE I     NASA
      DIMENSION A(8,25),CUT(25),XF(8)
      READ(5,7) N,M,BPHPS,BPLPS,(CUT(I), I=1,N),(XF(J),
     1J=1,M),XCO2P, XO2P, TEMP
    7 FORMAT (I5, I5, 4F15.5/(5F15.5))
      ALPHA = XCO2P/XO2P
      DELP = BPHPS - BPLPS
      DO 8 J=1,M
      DO 8  I=1,N
      VARA = (ALPHA -1.)*(BPLPS+CUT(I)*DELP)
      VARB = (ALPHA-1.)*(-BPHPS*XF(J)-CUT(I)*DELP)-DELP
     -ALPHA*BPLPS
      VARC = ALPHA*BPHPS*XF(J)
      Y=SQRT((-VARB)**2.-4.*VARA*VARC)
    8 A(J,I) = (-VARB-Y)/(2.*VARA)
      WRITE(6,9) ALPHA,DELP,TEMP,((A(J,I),J=1,M),I=1,N)
    9 FORMAT (1H 3F15.5//(8F15.5))
      CALL EXIT
      END
```

TABLE 17

OBJECT PROGRAM IS BEING ENTERED INTO STORAGE

ALPHA = 4.83819 DELP = 750.00000 TEMP = 25.00000

Cut Φ	X_F = 0.2000	X_p 0.10000	X_p 0.05000	X_p 0.01000	X_p 0.00100
0.9	0.21600	0.10827	0.05419	0.01085	0.00108
0.8	0.23454	0.11797	0.05914	0.01185	0.00119
0.7	0.25617	0.12951	0.06506	0.01306	0.00131
0.6	0.28156	0.14341	0.07227	0.01454	0.00146
0.5	0.31151	0.16040	0.08122	0.01640	0.00164
0.4	0.34679	0.18153	0.09260	0.01879	0.00189
0.3	0.38799	0.20823	0.10746	0.02200	0.00221
0.2	0.43506	0.24239	0.12753	0.02651	0.00267
0.1	0.48675	0.28625	0.15563	0.03329	0.00338
0.01	0 53498	0.33539	0.19148	0.04308	0.00443
0.001	0.53979	0.34081	0.19579	0.04438	0.00457
0.0001	0.54027	0.34136	0.19623	0.04451	0.00459

NOMENCLATURE FOR COMPUTER PROGRAM

BPHPS = Barometric pressure on the high pressure side of the membrane. mm Hg

BPLPS = Barometric pressure on the low pressure side of the membrane. mm Hg

CUT = Cut (Φ) or Fraction of feed gas permeated.

XF = Mole fraction of CO_2 in feed gas.

XCO2P = CO_2 permeability coefficient for silicone rubber at the separation temperature.

XO2P = O_2 permeability coefficient for silicone rubber at the separation temperature.

TEMP = Temperature at which the separation will take place.

ALPHA = Separation ratio (α).

DELP = Pressure drop across the membrane (ΔP).

VARA = The variable (a) of the quadratic equation.

VARB = The variable (b) of the quadratic equation.

VARC = The variable (c) of the quadratic equation.

A(I,J) = The product composition X_p obtained using CUT (I), and feed composition XF(J).

BIBLIOGRAPHY

1. American Society for Testing Materials, "Standard Method for Gas Transmission Rate of Plastic Sheeting", ASTM D 1434 - 58
2. Brubaker, D. W. and Kammermeyer, K.: Ind. Eng. Chem. 44, 1465 -74 (1952)
3. Kammermeyer, K.: Chem. Eng'g. Progress Symposium Series 55, No. 24, 115-25
4. Kammermeyer, K.: Ind. Eng. Chem. 49, 1685, (1952)
5. Major, C. J.: Modern Pkg. 36, (5), 119-122, June (1963)
6. Major, C. J. and Kammermeyer, K.: Modern Plastics, 39 (11) 135-146 179-180 July (1962)
7. Major, C. J.: "Interim Technical Report No. 1", NASA Contract # NASr-73
8. McIntosh, James R.: "Diffusion, Permeation and Solution of Selected Gases in Silicone Rubber", M. S. Thesis, State University of Iowa 1936
9. Mitchell, J. V.: Journal Roy. Inst. 2, 101, 301, 307 (1831)
10. National Aeronautics and Space Administration, Contract #NASr-73
11. Roberts, R. W.: "Effect of Polymeric Structure Upon Gas Permeation" Ph.D. Dissertation, State University of Iowa (1962)
13. Weller, S. W. and Steiner, W. A.: Journal Applied Physics, 21, 279-83, 1950

BIBLIOGRAPHY
(Continued)

14. Weller, S. W. and Steiner, W. A.: United States Patent #2, 540, 151

PROJECT REPORTS

15. Major, C. J., "Project Research Proposal"

16. Major, C. J., "First Quarterly Status Report," No. NASr-73.

17. Major, C. J., "Second Quarterly Status Report," No. NASr-73.

18. Major, C. J., "Third Quarterly Status Report," No. NASr-73.

19. Major, C. J., "Fourth Quarterly Status Report," No. NASr-73.

20. Major, C. J., "Fifth Quarterly Status Report," No. NASr-73.

21. Major, C. J., "Sixth Quarterly Status Report," No. NASr-73.

22. Major, C. J., "Seventh Quarterly Status Report," No. NASr-73.

23. Major, C. J., "Eighth Quarterly Status Report," No. NASr-73.

24. Major, C. J., "Ninth Quarterly Status Report," No. NASr-73.

25. Major, C. J., "Tenth Quarterly Status Report," No. NASr-73.

26. Major, C. J., "Eleventh Quarterly Status Report," No. NASr-73.

27. Major, C. J., "Twelfth Quarterly Status Report," No. NASr-73.

28. Major, C. J., "Thirteenth Quarterly Status Report," No. NASr-73.